Special Technical Report 34

MEASUREMENTS OF ELECTRON CONTENT AND LATITUDINAL F-LAYER CRITICAL FREQUENCY NEAR THE MAGNETIC EQUATOR

By: VICHAI T. NIMIT

Prepared for:

U.S. ARMY ELECTRONICS COMMAND
FORT MONMOUTH, NEW JERSEY 07703

CONTRACT DA 36-039 AMC-00040(E)
ORDER NO. 5384-PM-63-91

STANFORD RESEARCH INSTITUTE
MENLO PARK, CALIFORNIA

STANFORD RESEARCH INSTITUTE
MENLO PARK, CALIFORNIA

December 1967

Special Technical Report 34

MEASUREMENTS OF ELECTRON CONTENT AND LATITUDINAL F-LAYER CRITICAL FREQUENCY NEAR THE MAGNETIC EQUATOR

Prepared for:

U.S. ARMY ELECTRONICS COMMAND
FORT MONMOUTH, NEW JERSEY 07703

CONTRACT DA 36-039 AMC-00040(E)
ORDER NO. 5384-PM-63-91

By: VICHAI T. NIMIT

SRI Project 4240

Approved: E. L. YOUNKER, TECHNICAL DIRECTOR
MRDC Electronics Laboratory, Bangkok

W. R. VINCENT, MANAGER
Communication Laboratory

D. R. SCHEUCH, EXECUTIVE DIRECTOR
Electronics and Radio Sciences

Sponsored by
ADVANCED RESEARCH PROJECTS AGENCY
ARPA ORDER 371
FOR THE
THAI-U.S. MILITARY RESEARCH AND DEVELOPMENT CENTER
SUPREME COMMAND HEADQUARTERS
BANGKOK, THAILAND

ABSTRACT

Faraday rotation data from Satellite S-66 were accumulated at the Electronics Laboratory of the Military Research and Development Center, Bangkok, Thailand from November 1964 through June 1967, a period of intermediate sunspot number (sunspot minimum condition at 1964/1965 and sunspot maximum condition at 1968/1969). These data provide a means of improving ionospheric frequency predictions for regions in Thailand remote from Bangkok (i.e., where no ionosonde data are available).

In this report, two methods of analysis--involving rotation rate and total number of rotations--are applied to the Bangkok observations. The rotation-rate method is used to determine the electron content when the angle between the ray path and geomagnetic field is 90° (transverse position). The total-rotations method is used to determine latitudinal variations of electron content of the equatorial ionosphere for the selected passes from a joint analysis of observations at three stations in Thailand--Songkhla, Bangkok, and Chiengmai.

The diurnal variation of the local electron content shows low early-morning values and high afternoon values, resulting in a large maximum-to-minimum ratio. A secondary maximum was observed during the nighttime. The diurnal and seasonal variations of electron content are examined together with the variation with solar activity as measured by the 10.7-cm solar radio flux.

The diurnal development and collapse of the equatorial anomaly in electron content is clearly seen from the total-rotations data. The Chapman equation is used for conversion of these total electron content values to peak electron density in order to compute the F-layer critical frequency (foF2) and its variation as a continuous function of latitude. The computed foF2 values are compared with those obtained from three ionosondes which were located at Songkhla, Bangkok, and Chiengmai, and the agreement is typically within 10 percent.

FOREWORD

The work described in this report was performed with the support, and using the facilities, of the Military Research and Development Center (MRDC) in Bangkok, Thailand. The MRDC is a joint Thai-U.S. organization established to conduct research and development work in the tropical environment. The overall direction of the U.S. portion of the MRDC has been assigned to the Advanced Research Projects Agency (ARPA) of the U.S. Department of Defense who, in 1962, asked the U.S. Army Electronics Command (USAECOM) and the Stanford Research Institute (SRI) to establish an electronics laboratory in Thailand to facilitate the study of radio communications in the tropics and related topics. The MRDC-Electronics Laboratory (MRDC-EL) began operation in 1963 [under Contract DA 36-039 AMC-00040(E)] and since that time the ARPA has actively monitored and directed the efforts of USAECOM and SRI. In Bangkok, this function is carried out by the ARPA Research and Development Field Unit (RDFU-T). The cooperation of the Thai Ministry of Defense and the Thailand and CONUS representatives of the ARPA and USAECOM made possible the work presented in this report.

CONTENTS

CONTENTS (Continued)

ILLUSTRATIONS

ACKNOWLEDGMENTS

The author gratefully acknowledges the assistance of Miss Daranee Patamasuit of the Bangkok office of Pacific Technical Analysis, Inc., Honolulu, Hawaii, in helping to prepare the computer program. Thanks are due E. Golton of Radio and Space Research Station, Slough, England for helpful discussions. Goddard Space Flight Center, National Aeronautics and Space Administration (NASA) supplied the Satellite S-66 ephemeris data. Finally, the author would like to thank C. L. Rufenach of ESSA, Boulder, Colorado for comments on a draft of this report.

BLANK PAGE

I INTRODUCTION

One of the major activities of communication research in equatorial areas is the study of the ionosphere. A recent phase of this effort is the study of the development and collapse of the equatorial anomalies in electron content and F-layer critical frequency--the equatorial anomaly is the name given to a region of unusually high value of electron concentration or critical frequency in the F-region of the ionosphere near the magnetic equator. To increase understanding of these ionospheric characteristics, records of the Faraday rotation on 40- and 41-MHz signals from the S-66 (Explorer 22) radio beacon satellite have been accumulated from November 1964 through June 1967 at the MRDC Electronics Laboratory[1-5]* in Bangkok, and at two remote sites located north and south of Bangkok during 1966 and 1967. The projection of a typical satellite path of descending pass on the earth over these sites is shown in Fig. 1. Data were collected for sites in the range of geographic latitude between about 7°N and 19°N.

The methods of analyzing the data on Faraday rotation of radio signals from a satellite are described in detail in a Special Technical Report, STR 14,[6] which reported the results of electron content over Bangkok and the equatorial anomaly during the period of sunspot minimum.

This report presents the results of electron-content measurements over Bangkok for a period of intermediate sunspot number (sunspot minimum condition at 1964/1965 and maximum condition at 1968/1969). The content is used to calculate the equivalent slab thickness and the mean scale height. In this report the diurnal development and collapse of the equatorial anomalies in electron content and F-layer critical frequency are analyzed from selected Faraday rotation data from satellite passes observed by the receiving stations Songkhla, Bangkok, and Chiengmai. Using the Chapman equation, the electron content data are used to calculate the F-layer critical frequency of the equatorial ionosphere. The assumptions involved are given, and the possible sources of error due to those approximations are discussed.

*References are listed at the end of the report.

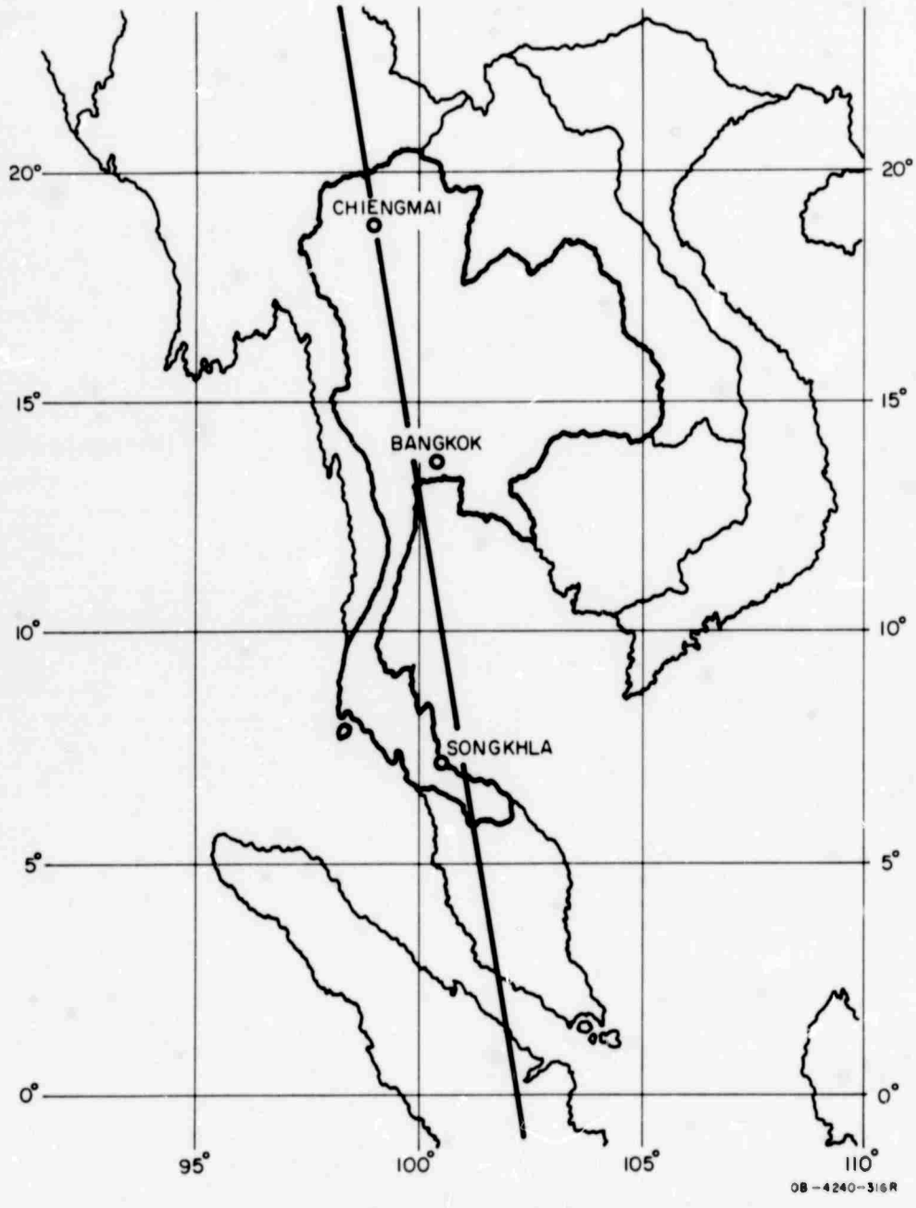

FIG. 1 LOCATION OF SATELLITE RECEIVING SITES

II THEORETICAL BACKGROUND

When a linearly polarized electromagnetic wave is propagated through a low-loss, ionized medium, such as the ionosphere, and is under the influence of the earth's magnetic field, the polarization of the resultant electric field vector rotates gradually as the wave moves through the ionosphere. This phenomenon is commonly referred to as Faraday rotation.

The relationships between a satellite and a ground observation point are shown in a simplified form in Fig. 2. The important angular

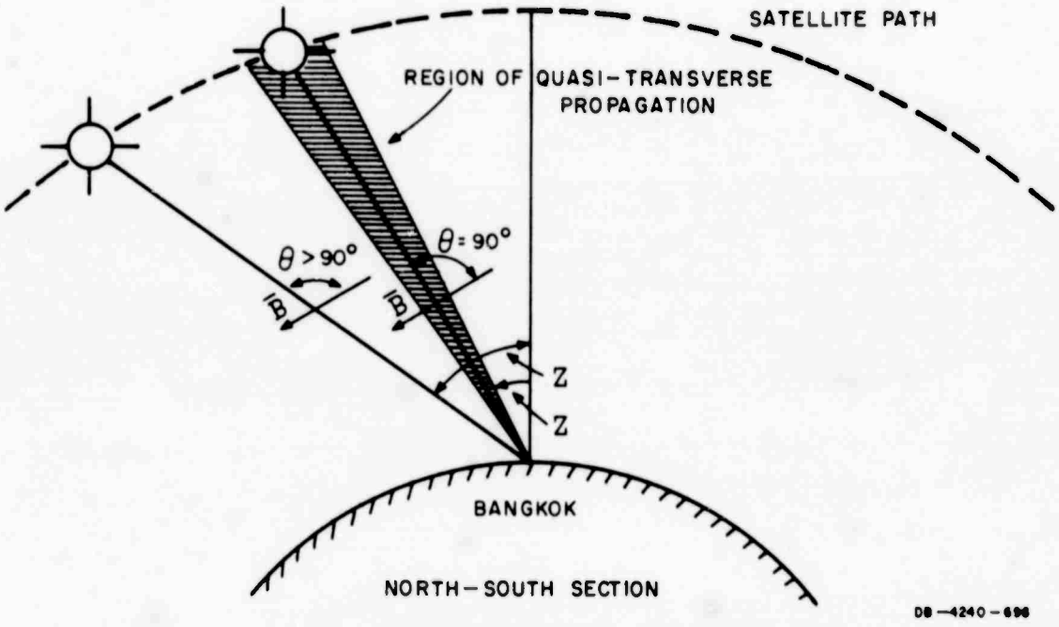

FIG. 2 FARADAY ROTATION GEOMETRY

parameters are Z, the satellite zenith angle (the angle between the signal ray path and the vertical), and θ, the angle between the signal ray path and the earth's magnetic field. Two positions of the satellite are indicated--the usual case, where $\theta \neq 90^\circ$, and a special case, where $\theta = 90^\circ$. The region near $\theta \approx 0^\circ$ is called the region of quasi-longitudinal (QL)

propagation, and the point where $\theta = 0^o$ is called longitudinal case. The region near $\theta \approx 90^o$ is called the region of quasi-transverse (QT) propagation, and the point where $\theta = 90^o$ is called the transverse case or T_o position. (At this point the sense of rotation will be reversed.)

A linearly polarized signal can be treated as the sum of two circularly polarized waves with opposite directions of rotation. It can be shown that the angle of the plane of polarization rotates as the wave travels through the ionosphere.

Using Ratcliffe's[7] notation and defining the complex refractive index as:

$$n = \frac{k}{k_o}$$

where

$k_o = \frac{2\pi}{\lambda_o}$ = Phase constant in free space

λ_o = Radio Wavelength in free space

$k = \frac{2\pi}{\lambda}$ = Phase constant in medium

λ = Radio wavelength in the medium

$k_e = n_e k_o$ = Ordinary (left-hand polarization) component phase constant

$k_r = n_r k_o$ = Extraordinary (right-hand polarization) component phase constant.

From the geometry illustrated in Fig. 3, propagation is in the z direction and an element of path length in this direction is $d\ell$. The change in angle of polarization rotation, $d\Omega$, as the wave proceeds a distance $d\ell$, is given by:

$$d\Omega = \frac{k_o}{2} (n_e - n_r)\, d\ell \qquad (1)$$

where the resultant electric field of the wave is

$$E = E_e e^{ik_e z} + E_r e^{ik_r z} \quad .$$

In the quasi-longitudinal case, the Appleton-Hartree equation for the refractive index under the QL approximation is

$$n_{e,r} \approx 1 - \frac{X}{2} \pm \frac{XY_L}{2} \tag{2}$$

and

$$d\Omega = \frac{k_o}{2} (XY_L) d\ell \tag{3}$$

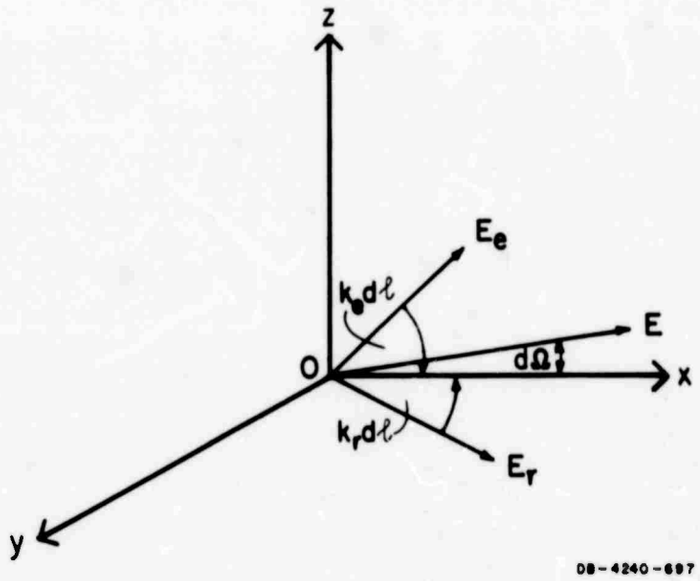

FIG. 3 VECTOR GEOMETRY

In terms of mks units,

$$d\Omega = \frac{K}{f^2} NH_o \cos\theta \, d\ell \tag{4}$$

where

H_o = Earth's magnetic field intensity, amp-turn/m

N = Electron density, electron/m^3

f = Frequency of satellite transmission, Hertz

K = A constant = 2.97×10^{-2}, mks units

Ω = Angle of polarization rotation, radian

$d\ell$ = Element of path length

θ = Angle between the magnetic field and wave normal (direction of propagation).

To find the electron content in a vertical column (vertical columnar electron density) through the ionosphere, it is convenient to replace the path element $d\ell$ by dh sec χ, where χ is the local zenith angle and dh is an element height. With this substitution, Eq. (4) becomes

$$d\Omega = \frac{K}{f^2} NH_o \cos\theta \sec\chi \, dh \quad . \tag{5}$$

Integrating over height from zero to the satellite height,

$$\Omega = \frac{K}{f^2} \int_o^{h_s} NH_o \cos\theta \sec\chi \, dh \quad . \tag{6}$$

The total number of rotations of the plane of polarization of the linearly polarized resultant is

$$R = \frac{\Omega}{2\pi}$$

$$= \frac{K}{2\pi f^2} \overline{H_o \cos\theta \sec\chi} \int_o^{h_s} Nd'h \tag{7}$$

$$= \frac{Q}{f^2} \overline{B \cos\theta \sec\chi} \int_o^{h_s} Ndh \tag{8}$$

where

Q = A constant = 3.77×10^{-13}, mks units

f = Frequency, MHz

B = Earth's magnetic intensity, Gauss

$\overline{B \cos\theta \sec\chi}$ = A weighted mean over the range of integration;

or, more compactly,

$$R = G \int Ndh \quad . \tag{9}$$

In order to determine the electron content using Eq. (9), the value of G may be calculated* at any point in the spatial coverage around the observer. In general, the G value must be the weighted average of the actual value of B cos θ sec χ along the line of the ray path. By using the average ionospheric profile, the value of G is determined near the

*The calculation of G values is given in Appendix A.

height of the centroid of the ionospheric electron-density profile. The centroid height for the area of interest is obtained by fitting the Faraday rotation electron content data to the ionospheric distribution profile. Therefore, the value of G is evaluated at a level approximately 50 km above the height of maximum density,[8] which can be determined from a true-height analysis of vertical-incidence ionograms obtained near the location and time of the satellite passages.

Equation (9) was derived under the following assumptions:

(1) The wave frequency is so high that refraction can be neglected. (That is, the wave frequency is much higher than the maximum plasma and collision frequencies.)

(2) The effect of horizontal electron gradients can be neglected.

(3) The quasi-longitudinal approximation holds.[7]

(4) The vertical velocity component of the satellite can be neglected.

(5) The satellite antenna has a fixed spatial orientation.

(6) A single ray path exists for both modes.

Equation (9) is a good approximation to a more exact formula as long as the quasi-longitudinal approximation is valid. The quasi-longitudinal approximation is not valid near $\theta = 90^{\circ}$, the transverse position (which occurs at the time T_o). At $\theta = 90^{\circ}$, both R and G in Eq. (9) go to zero and the expression for electron content becomes indeterminate. It is realized that at the transverse point the rotation is a complicated series of polarization changes. The method used to obtain the electron content at the transverse position is a method of interpolation--the rotation-rate method. To obtain the rotation rate, Eq. (9) is differentiated with respect to time, giving

$$\frac{dR}{dt} = \int_o^{h_s} Ndh \cdot \frac{dG}{dt} + G \cdot \frac{d}{dt} \int_o^{h_s} Ndh \quad . \qquad (10)$$

When the horizontal gradients in the ionosphere are neglected for a very narrow latitudinal range of the ionosphere, the second term

becomes zero. Therefore, the rotation rate becomes proportional to the electron content

$$\frac{dR}{dt} = \frac{dG}{dt} \int_o^{h_s} Ndh \tag{11}$$

thus

$$\int_o^{h_s} Ndh = \frac{\dot{R}}{\dot{G}} \quad . \tag{12}$$

In Eq. (12) the dot implies a time derivative. The $\dot{G}$ can be determined indirectly by differenting the G with respect to time, to obtain

$$\dot{G} = \frac{dG}{dt} \tag{13}$$

$$= \frac{dG}{d\theta_s} \cdot \frac{d\theta_s}{dt} \tag{14}$$

where θ_s is satellite latitude and $\frac{d\theta_s}{dt}$ is the time derivative of satellite latitude. Near the geographic equator, for Satellite S-66 at a height of 1000 kilometers, $\frac{d\theta_s}{dt}$ has the value 0.0565 degrees per second.

Equations (9) and (12) are the basic relationships for calculating electron content from experimentally obtained Faraday rotation data.

III METHOD OF ANALYSIS

A. GENERAL APPROACH

One widely used method of studying the electron distribution in the ionosphere is the Faraday rotation technique. The principal advantage of the Faraday rotation technique for calculating electron content used in this study is the simplicity of data acquisition and analysis. Analysis of Faraday rotation data can be done in two ways--by the rotation-rate method and by the total-rotations method. The rotation-rate method is suitable for analyzing a large number of records and has the advantage of being relatively insensitive to horizontal gradients of electron content. However, it can be used only in calculations of electron content near the transverse position and so can give values at only one location. The rotation-rate method has been applied to Bangkok data. The total-rotations method is more complex but has the advantage of yielding values of electron content over a range of latitudes. This method is easy to use for data from a station near the magnetic equator, because the usual polarization-rotation ambiguity can be resolved when the satellite passes through the T_o position. By counting the number of rotations of the plane of polarization from this transverse point, one is able to determine an unambiguous measurement of electron content for latitudinal variation. The total-rotations method was applied to the data from the three-station chain--Songkhla-Bangkok-Chiengmai.

Figure 4 gives an example of the appearance of the Faraday polarization fading-rate anomaly on signal-amplitude records which were observed at three stations during a typical passage of Satellite S-66. These Faraday fading data were recorded on 40 MHz for the purpose of determining the latitudinal variation of electron content over Thailand. The fading pattern seen in Fig. 4 is caused by the resultant polarization vector of the received signal alternately falling parallel to and orthogonal to the linearly polarized antenna. Since the signal polarization (electric field intensity) vector becomes parallel with the dipole twice during each rotation of 360°, a complete rotation corresponds to two

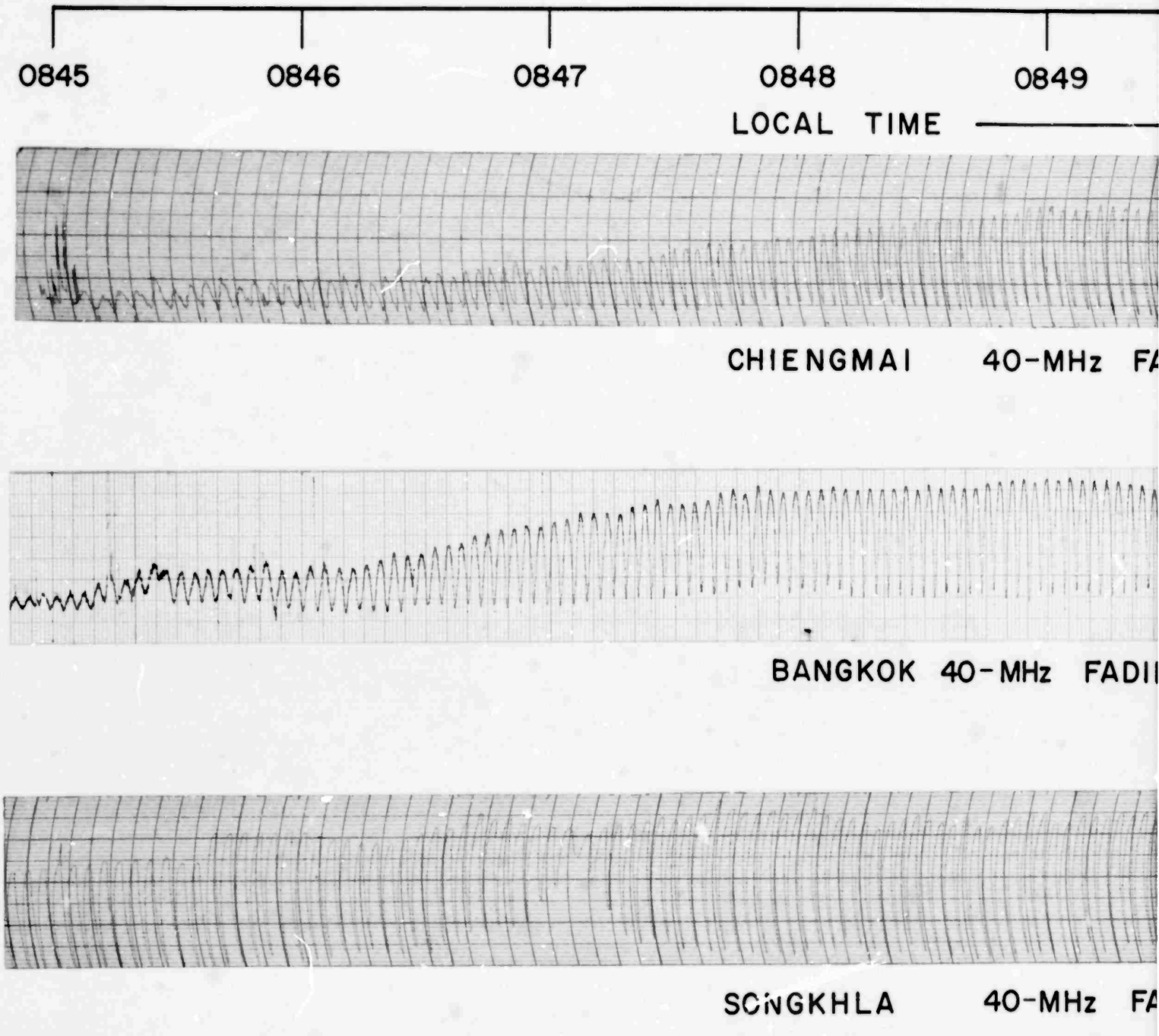

FIG. 4 SAMPLE S-66 SATELLITE SIGNAL-AMPLITUDE REC
26 FEBRUARY 1967, REVOLUTION NUMBER 11939, A

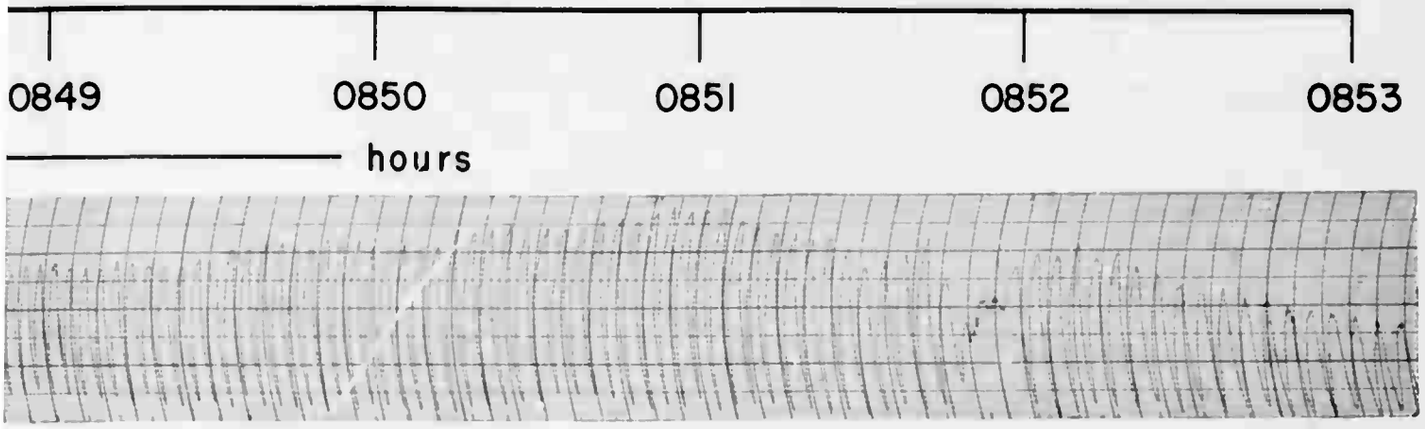

)-MHz FADING RECORD

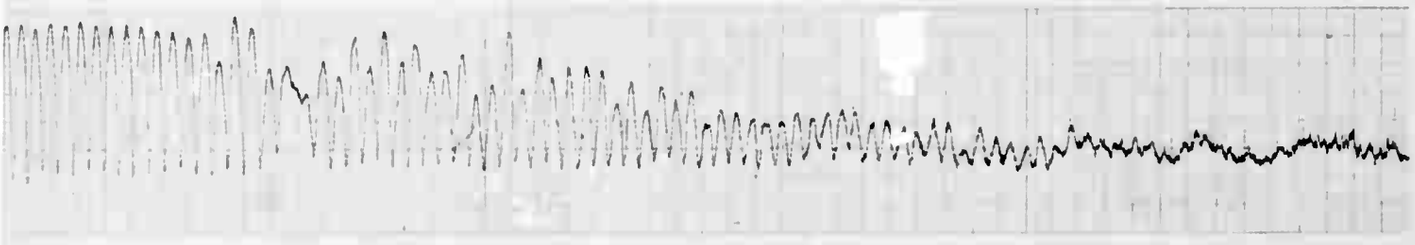

MHz FADING RECORD

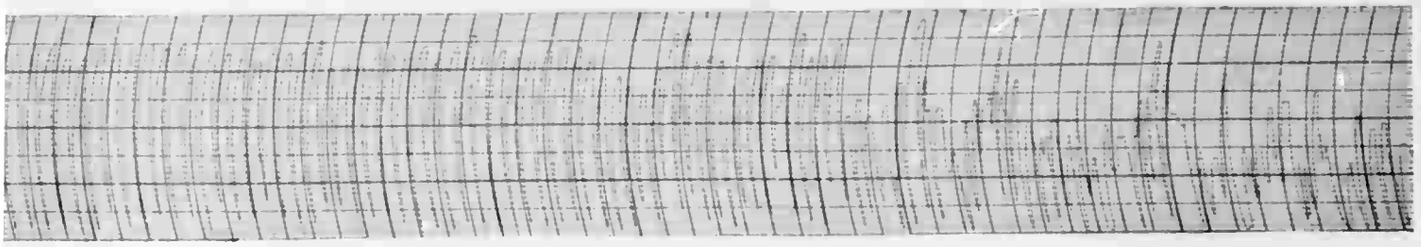

)-MHz FADING RECORD

D-4240-1807

AMPLITUDE RECORDINGS FOR THREE STATIONS —
NUMBER 11939, ASCENDING PASS

FIG. 4

periods of the fading pattern. The unique point--the time of occurrence of transverse propagation T_o--is plainly visible in Fig. 4. The change in the pattern near T_o is caused by the reversal in the direction of the polarization vector rotation. Local time* was recorded on the chart to relate the observed data to the physical position of the satellite in its orbit. The satellite position and height at time corresponding to the local time were obtained from ephemeris data provided by the U.S. National Aeronautics and Space Administration (NASA).

B. ROTATION-RATE METHOD

The rotation-rate method of analysis is based on the rate of change of rotation near the T_o position to determine the electron content at that position. In this method of analysis, Eq. (12) is used to obtain the electron content. In this equation, $\dot{R}$ can be measured directly from the data by graphical calculation. The $\dot{G}$ coefficient is determined by differentiating G as shown by Eq. (14). The calculation has been prepared for computer calculations.

A typical plot of the number of rotations observed on a record is shown in Fig. 5. The number of rotations (left-hand scale) is counted, starting from an arbitrary first null of the signal amplitude in the Faraday rotation record, and the time corresponding to the third, fifth, etc., nulls are used to plot the number of rotations as a function of local time. Figure 5 illustrates the calculation of the rotation rate, $\dot{R}$, by a three-point numerical differentiation method (using the slope of the curve near T_o). The number of rotations is scaled from a 1-minute period centered at the T_o position. This gives the rotation rate ($\dot{R}$) directly in rotations per minute. The ratio of the rotation rate ($\dot{R}$) to the coefficient ($\dot{G}$) yields the electron content as given in Eq. (12).

---

*Local time (GMT + 7 hours) was established using a General Radio 115B Frequency Standard adjusted using phase referenced to the VLF transmission from GBR in England on 15 kHz. Time ticks generated by a GR 1123A Syncronometer from this standard were compared daily with time transmission from WWVH and JJY on 10 and 15 MHz. The resulting time estimate is accurate to 5 milliseconds.

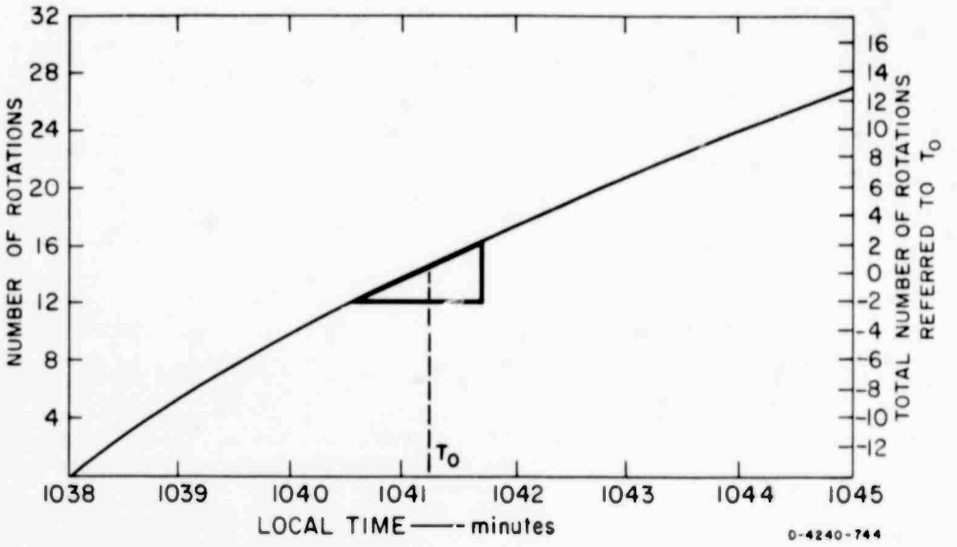

FIG. 5 SAMPLE ANALYSIS CALCULATION

C. TOTAL-ROTATIONS METHOD

For a station near the magnetic equator, ambiguity in the total number of rotations can be resolved easily for most records. There is a time during each satellite passage when transverse propagation occurs and the resulting reversal of wave polarization produces a visible perturbation of the Faraday fading pattern at that time (T_o). The total number of rotations is defined as equivalent to zero at the T_o position. The total-rotations method of analysis uses the total number of rotations from the transverse position to a given satellite position to determine the electron content at that position. The right-hand scale of Fig. 5 illustrates the total number of rotations referred to T_o for different times during a satellite pass. The total number of rotations is counted from T_o to the time corresponding to the satellite latitude on both sides of T_o. Satellite S-66 has a nearly polar orbit; hence the satellite latitude is a more sensitive variable in this analysis.

To follow the above procedure, the local time corresponding to the satellite position must be known accurately. The satellite ephemeris is used to tabulate the different satellite positions corresponding to

local time during the observation period. The total number of rotations (R) is counted from the right-hand scale in Fig. 5 and the corresponding satellite position is obtained from the local-time tabulations of the satellite ephemeris. In this method of analysis, Eq. (9) is used to obtain the latitudinal electron content. A computer program has been prepared for this analysis that can be used to compute the latitudinal variation of electron content for any satellite passage of interest (see Appendix B).

IV RESULTS

A. LOCAL ELECTRON CONTENT

The local electron content over Bangkok was calculated by using Eq. (12) at the transverse position. This position corresponds to the ionospheric point of approximately 14.2°N latitude for all satellite passes recorded. The electron content values presented in this section have been calculated from the Faraday rotation data obtained from Satellite S-66 from November 1964 through June 1967, a period of intermediate sunspot number (sunspot minimum condition at 1964/1965 and maximum condition at 1968/1969).

To see the main features, the electron content was plotted for the ascending and descending passes separately, as shown in Figs. 6 and 7 respectively. Because the satellite precessed westward, the time of the satellite passage over Bangkok became progressively earlier. No difference is apparent between the results for the two directions of passage. The time of day advances from right to left in Figs. 6 and 7, and each calculated value of electron content is associated with a particular hour of the day. Therefore, the passage time moved through a 24-hour period in about five and a half months.

In addition to the calculated values of electron content, F-layer peak electron density and the daily mean 10.7-cm solar flux values are shown in Figs. 6 and 7. In these figures, the top curve is the electron content, the middle curve is the F-layer peak electron density calculated from the ionosonde observations over Bangkok, and bottom curve shows the daily mean 10.7-cm solar flux. The main feature of the electron content results is the large diurnal variation--low early morning and high afternoon values. The maximum value of electron content varied from 20×10^{16} electron/m^2 at the low sunspot number (February 1965) to 55×10^{16} electron/m^2 at high sunspot number (March-April 1967) and occurred around 1400 hours local time, while the minimum value of electron content varied from 1×10^{16} electrons/m^2 at the low sunspot

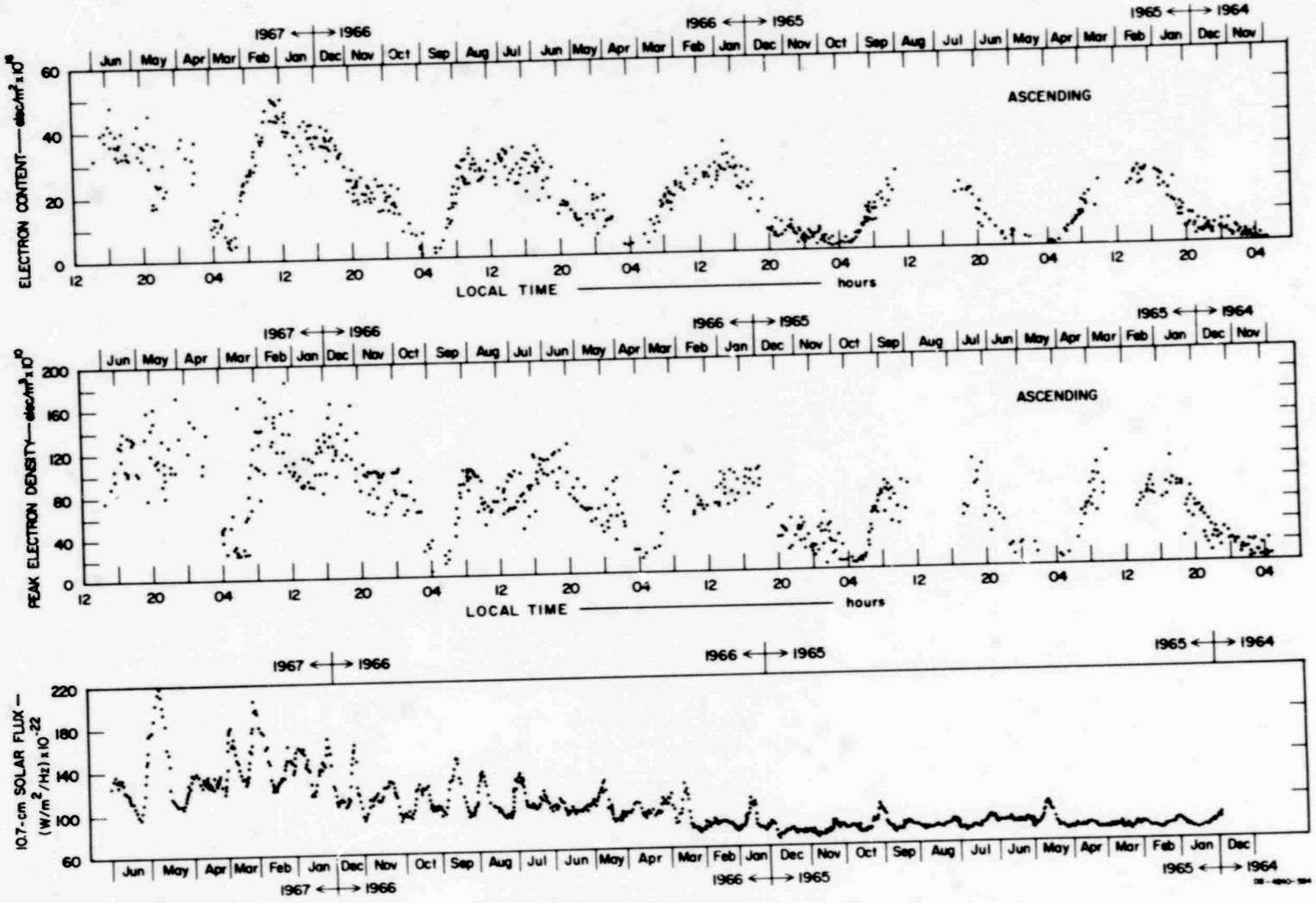

FIG. 6 DIURNAL VARIATION OF ELECTRON CONTENT AND F-LAYER PEAK ELECTRON DENSITY AND SOLAR FLUX — ASCENDING PASSES

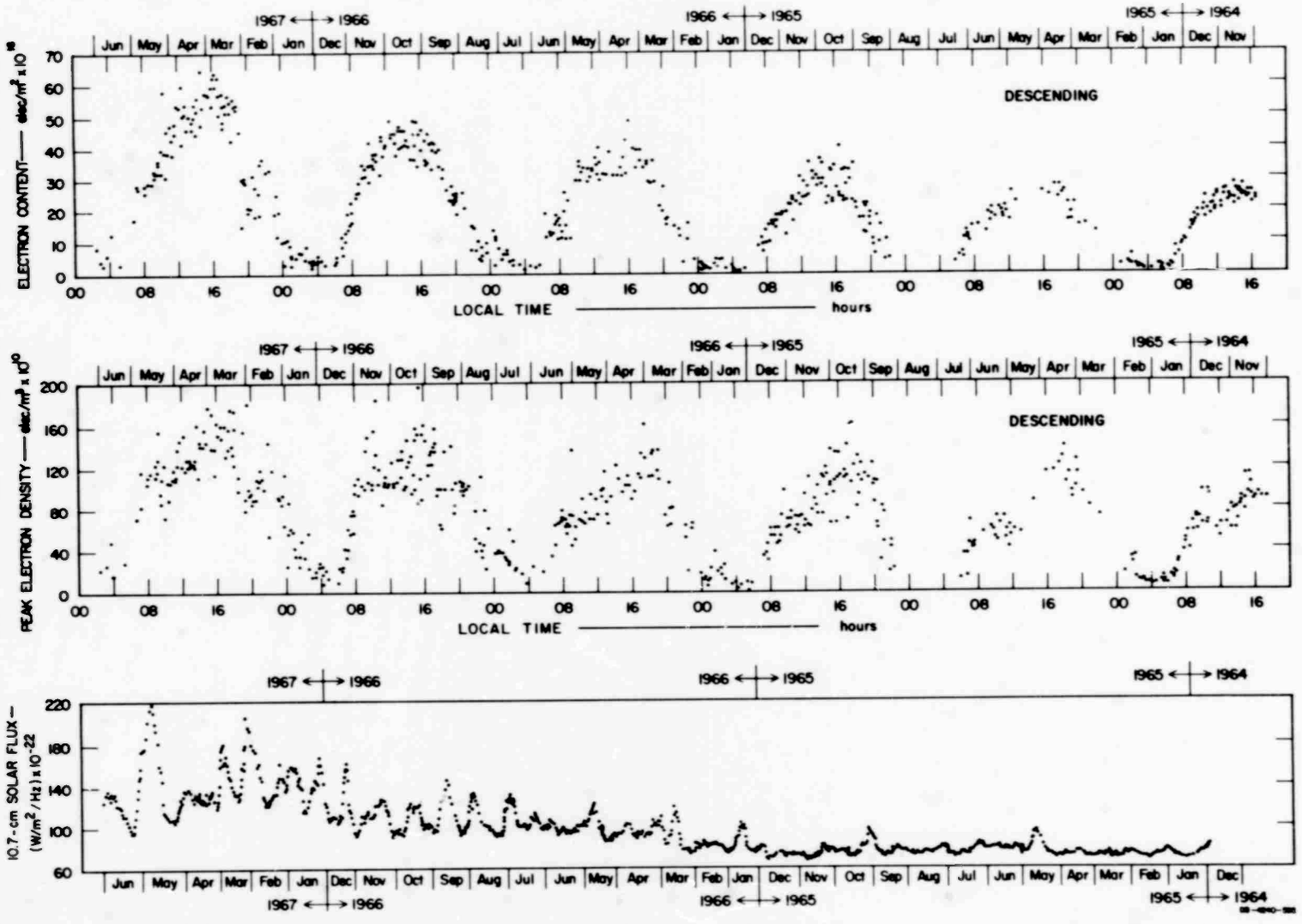

FIG. 7 DIURNAL VARIATION OF ELECTRON CONTENT AND F-LAYER PEAK ELECTRON DENSITY AND SOLAR FLUX — DESCENDING PASSES

number (January-February 1965), to 10×10^{16} electron/m^2 at the high sunspot number (March 1967), and occurred in the early morning hours. The slope of the diurnal curve rose sharply in the morning hours, reached a peak in the afternoon, and decayed rapidly to a minimum in the early morning hours. Secondary maxima were observed at the nighttime hours. This nighttime behavior of ionospheric electron content agrees with the observations by other investigators at other latitudes.[9-12]

The values of the F-layer peak electron density (see Figs. 6 and 7) were calculated from ionosonde data obtained at times very nearly corresponding to the satellite passes. The curves of electron content and peak electron density are generally somewhat similar. It is noticeable that the secondary maximum of peak electron density also appeared at nighttime. The cause of these secondary maximum values is not clear.

Solar flux values (10.7 cm) are plotted in Figs. 6 and 7 as an index of solar ultraviolet activity during the period of satellite (and vertical-incidence-sounder) ionospheric observations. The main features are the diurnal variations of solar flux, which show a correlation with the envelope of the peak electron content values.

B. SEASONAL VARIATIONS

It is apparent in Figs. 6 and 7 that the diurnal variations shown in these plots are contaminated by seasonal variations. The seasonal variations of the daytime maximum values of electron content are illustrated in Fig. 8. In order to study this variation further, the daytime maximum electron content values during sunspot number minimum in 1964 are taken from Ref. 6.

The principal features are the low electron content value during the sunspot minimum in 1964, and the electron content increasing as the sunspot number increases toward maximum. The seasonal variation in Fig. 8 shows the maximum values of electron content occurring near the March-April and September-October equinoctial periods, since in this period the sun is directly overhead at the equator, and minimum values occurring near June-July and December-January of solstitial periods.

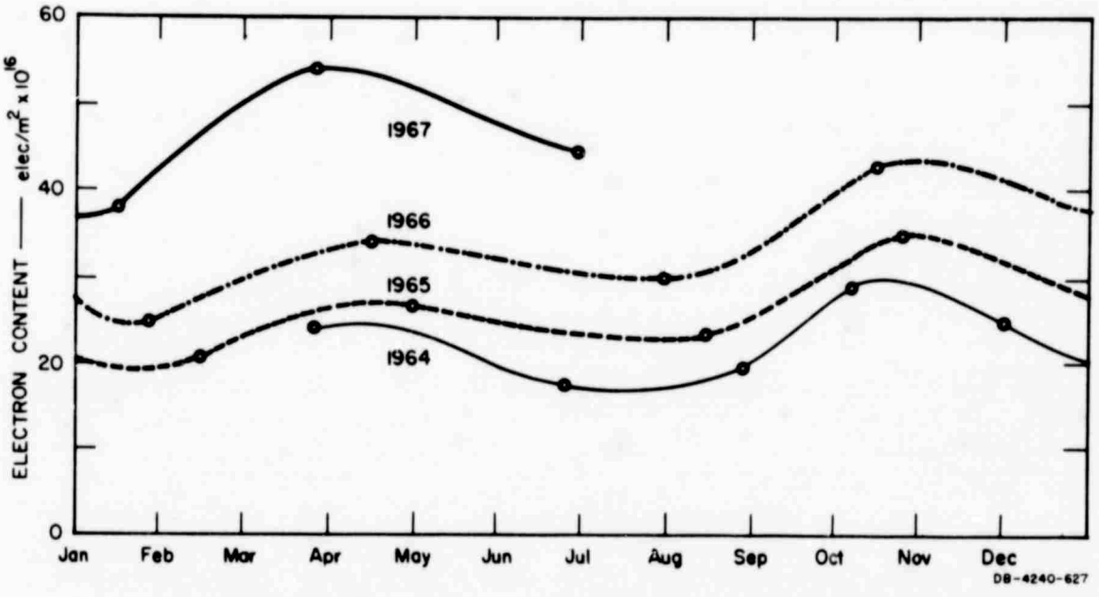

FIG. 8 SEASONAL VARIATION OF PEAK ELECTRON CONTENT

C. SOLAR VARIATIONS

To investigate the dependence of electron content upon solar activity, the values of electron content during the middle of the day (Figs. 6 and 7), when the diurnal rate of change is small, are plotted against the corresponding daily mean 10.7-cm solar flux values (see Fig. 9). In Fig. 9 the lower points are for the low sunspot number period and the upper points are for the high sunspot number period. This indicates an increase of electron content with solar flux that is the same order of magnitude as the effect of sunspot number. Apparently the electron content is linearly dependent upon solar flux, at least for small-to-moderate values of solar flux.

D. SLAB THICKNESS AND SCALE HEIGHT

The slab thickness and mean scale height of the ionosphere are closely related to the electron distribution profile. They can be computed from the following equations:[13,14]

$$\int Ndh = 4.13\ \bar{H}\ (N_{max}F) \qquad (15)$$

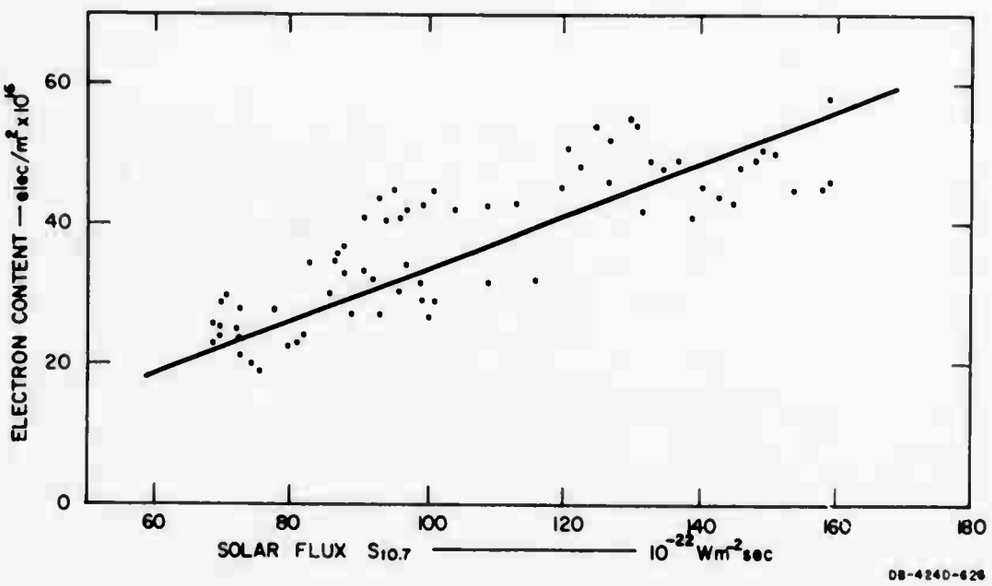

FIG. 9 SOLAR VARIATION OF PEAK ELECTRON CONTENT

where

$$\overline{H} = \frac{\int_o^{h_s} H(h)\, dh}{h_s}$$

$H(h)$ = Scale height

$\overline{H}$ = Mean scale height

h_s = Satellite height

$N_{max}F$ = Peak electron content of the F-layer.

By definition, the total electron content is equal to the product of equivalent slab thickness and peak F-layer electron content. Therefore, the equivalent slab thickness can be identified as $4.13\,\overline{H}$ in Eq. (15).

It is evident that the mean scale height and slab thickness are related by a factor of 4.13. The individual value of electron content, determined by the rotation-rate analysis, can be divided by the peak electron density ($N_{max}F$) obtained from ionosonde data taken at the same time to obtain the equivalent slab thickness. The peak electron density can be obtained from ionospheric data collected at Bangkok by a modified C-2 ionosonde, by using the following relation:

$$N_{max}F = 1.24\ (foF2)^2 \times 10^{10} \qquad (16)$$

where foF2 is the observed F_2-layer ordinary wave critical frequency (megahertz), and $N_{max}F$ is the peak electron density (electron/m^3).

The diurnal and seasonal variation of slab thickness and mean scale height are clearly shown in Fig. 10. Data for the ascending and descending passes are plotted separately. In Fig. 10 a definite variation between day and night is discernible, since both slab thickness and mean scale height have the diurnal variation. The maximum daytime slab thickness and mean scale-height values vary between about 300 to 400 km and 75 to 100 km respectively. The minimum nighttime values of slab thickness and mean scale height range approximately from 120 to 190 km and 30 to 45 km, respectively. These values are generally comparable to other published values.[6]

E. ACCURACY OF RESULTS

The rotation-rate method is suitable for the analysis of a large number of recordings and is relatively insensitive to horizontal electron gradients near the transverse (T_o) position. It is obvious from Eq. (9) that a Faraday effect cannot be claimed to exist at the transverse position. The only method to obtain the electron content at the transverse position is the rotation-rate method. In the complete equation, Eq. (10), the second term (which is neglected for the rotation-rate analysis) increases the rotation rate when horizontal gradients are present. By using the horizontal gradients from the three-stations analysis of the selected passes, we have determined that the second term causes less than 5-percent error in the value of the rotation rate of the S-66 satellite signals.

In this study, the T_o time can be observed experimentally from the satellite passes. The accuracy of this observation was limited by the width of the recorder marking lines. The smallest division of time on the marking scale was 5 seconds. The events time record (see Fig. 4)

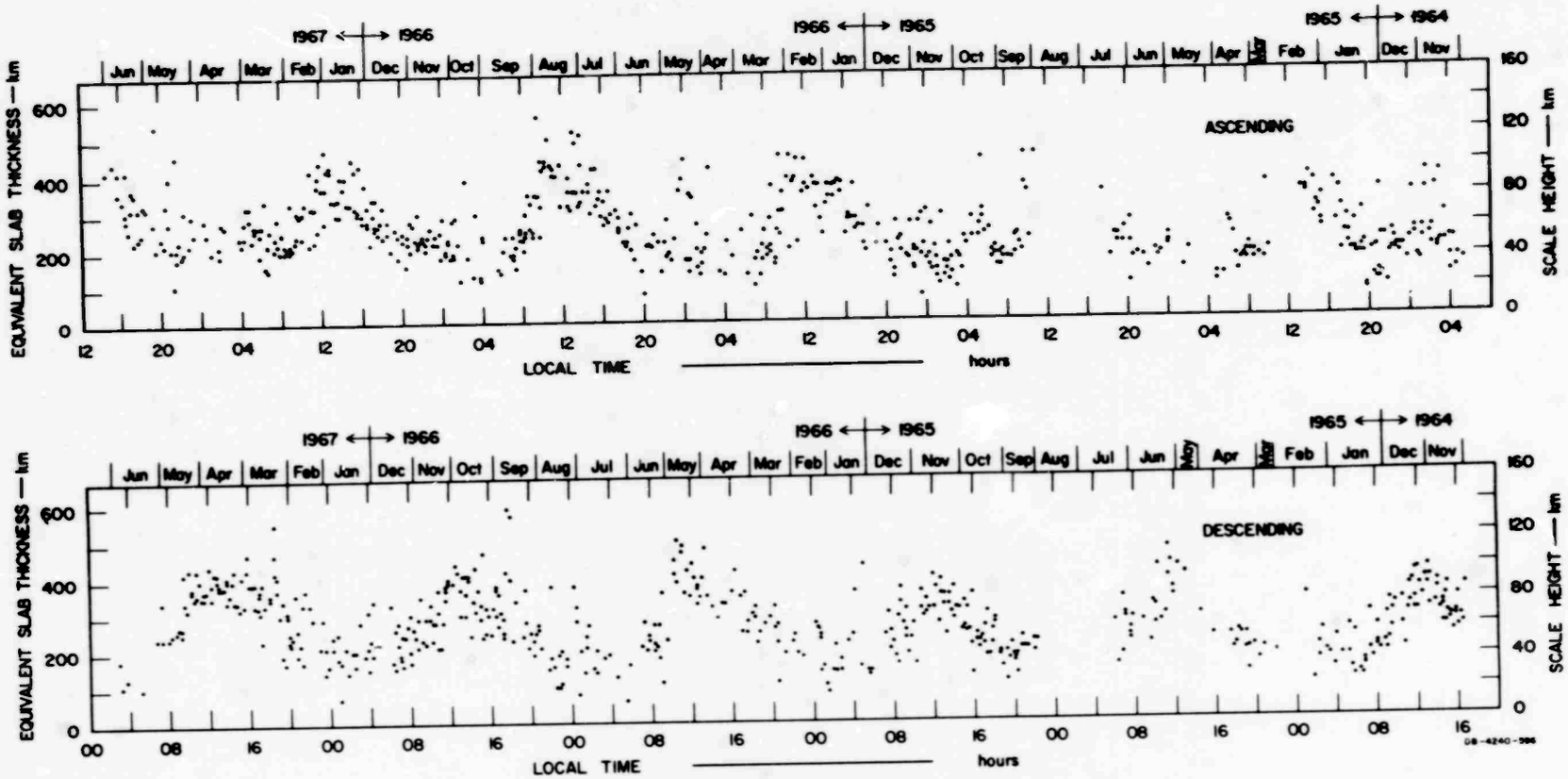

FIG. 10 DIURNAL VARIATION OF EQUIVALENT SLAB THICKNESS AND MEAN SCALE HEIGHT— ASCENDING AND DESCENDING PASSES

can be resolved to within 1 second. For the satellite passes with no other observable T_o time, the T_o time had to be calculated. When calculations are made for passes with observable T_o times, the calculated values of T_o are almost always within a few seconds of the observed values.

The total errors in the values of electron content derived from the rotation-rate are usually less than 10 percent. However, an exception occurs for the early morning hours, when the rate drops to less than 1 revolution per minute, which may cause errors as large as 20 percent.

BLANK PAGE

V DEVELOPMENT OF THE EQUATORIAL ANOMALIES

A. LATITUDINAL VARIATION OF ELECTRON CONTENT

The latitudinal variation of electron content is determined by the total-rotations method. A computer program has been prepared for Eq. (9) that is used to compute the latitudinal variation of electron content for the selected passes. The total number of rotations is measured from the transverse position to a given satellite position, and the corresponding satellite position is obtained from the local-time tabulations of the satellite ephemeris. From this calculation, the sub-ionospheric point (the projection on the earth of the intersection of the ray path between satellite and ground stations with the centroid of the ionospheric electron distribution profile) traversed about 10° of latitude around a ground station. Therefore, the latitudinal variation of electron content can be calculated for a section across the sky.

To increase the range of latitude over which the electron content could be investigated, two remote sites were set up at Chiengmai and Songkhla, which are located north and south of Bangkok respectively (Fig. 11). By analyzing data collected at these two remote stations as well as at Bangkok from November 1966 to March 1967, the electron content over a latitude range of more than 25° could be obtained. The selection of satellite fading records that would yield high quality for analysis at all three stations was governed by the following conditions:

(1) The satellite equatorial-crossing longitude for ascending passes should be between 98 and 107°E, and for descending passes should be between 93 and 102°E, because of the inclination of the satellite orbit and the locations of three stations.

(2) The data-recording period must be long enough to obtain data overlaping between Songkhla and Bangkok, and between Chiengmai and Bangkok.

(3) The fading records should be free of scintillation.

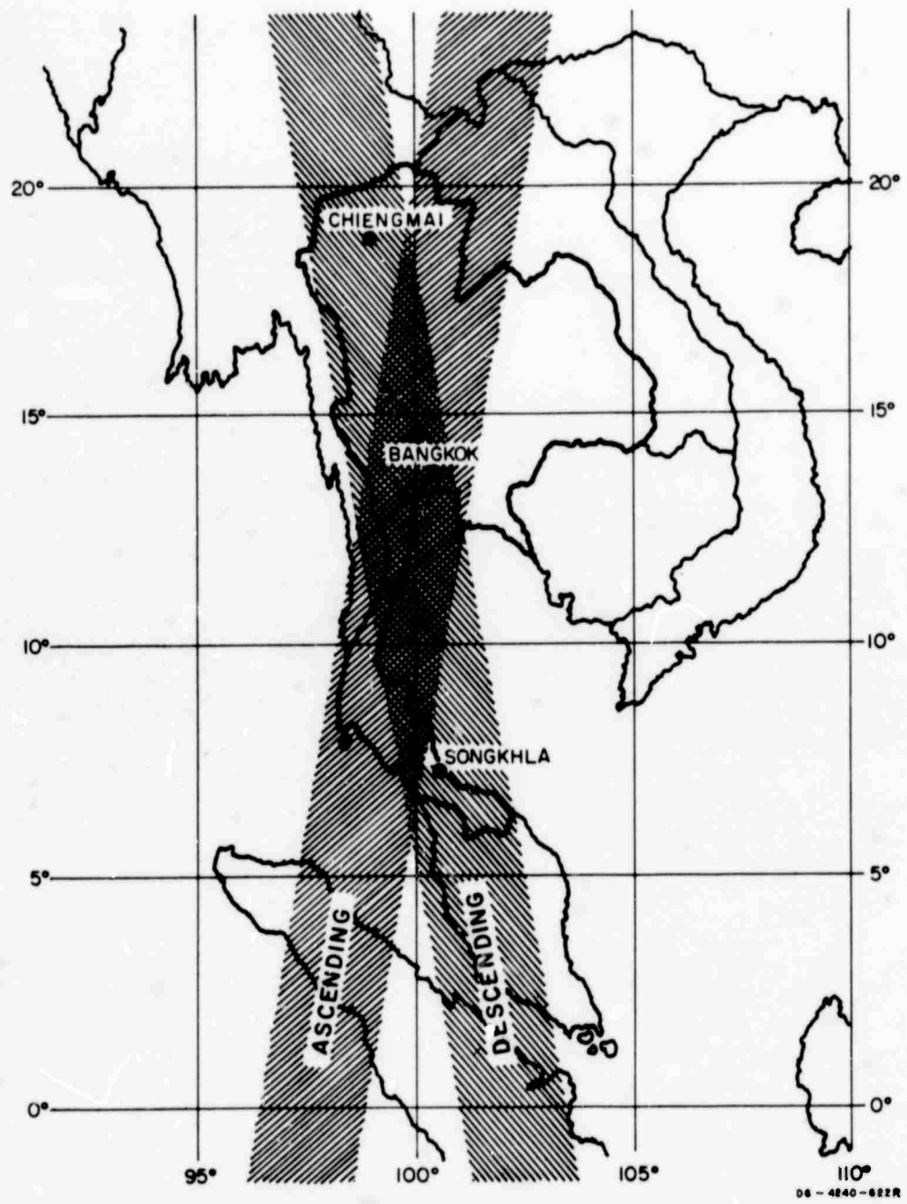

FIG. 11 SHADED ZONES OF SELECTED SUB-IONOSPHERIC PATH

The electron content was calculated for points along the sub-ionospheric path (the projection on the earth of the locus of the point at which the ray path between satellite and ground station intersects the centroid of the ionospheric electron-distribution profile). The sub-ionospheric paths for the selected passes all fall within the shaded zone shown in Fig. 11. The zones for ascending and descending passes are shaded separately. Records for which the electron content is calculated were selected from a period of November 1966 through March 1967. The satellite passes occur at different local times owing to the precession of the orbit; the times in this period are distributed covering twenty-four hours. Therefore, it is convenient to pool the selected passes on a time-block basis, in one-hour groups. Ephemeris data of the selected passes for each hour group are given in Appendix C.

The results of the latitudinal electron content of each hour group are presented in Part (a) of Figs. 12 through 32. The number beside each curve is a key to the data on which the satellite pass occurred; the date can be determined by reference to Appendix D. Notice that the data for the local-time blocks 0300-0400, 0500-0600, and 1600-1700 are missing. This is because of the poor quality of the records and the lack of observations for analysis. The computed values of latitudinal electron content are plotted as a function of geographic latitude and magnetic dip angle. The principal features of the results show the diurnal development and collapse of the equatorial anomalies in the electron content. The latitudinal variations of electron content from the period 0000-0700 of local time showed a rather flat variation of latitudinal distribution, as illustrated in Part (a) of Figs. 12 through 16. These figures show that electron content at the southern location is higher than at the north. This effect is caused by the season when the Faraday fading records were obtained, since the records were observed for the period of winter solstice. The sun is south of the equator, so the expected higher values of electron content in the southern hemisphere are obtained. At the period 0800-1000 hours of local time, the latitudinal distribution of electron content is characterized by a peak near the

magnetic dip equator as illustrated in Part (a) of Figs. 17 and 19. The electron content variations demonstrate the general shape of the equatorial-trough anomaly as observed between 1000 and 1600 local time [Part (a) of Figs. 20 through 25]. The variations show a trough near the magnetic equator. The latitudinal variation of electron content is collapsed to a peak and shifted north of the magnetic equator near the sunset hour 1700-1800 local time as illustrated in Part (a) of Fig. 26, and the equatorial trough anomaly is developed again at period 1800-0000 local time as illustrated in Part (a) of Figs. 27 through 32. The exception of one peak of electron content near the magnetic equator as shown by Curve 1 in Part (a) of Fig. 29 is not well understood. This diurnal development and collapse of the equatorial anomalies has been reported by other workers.[15,16]

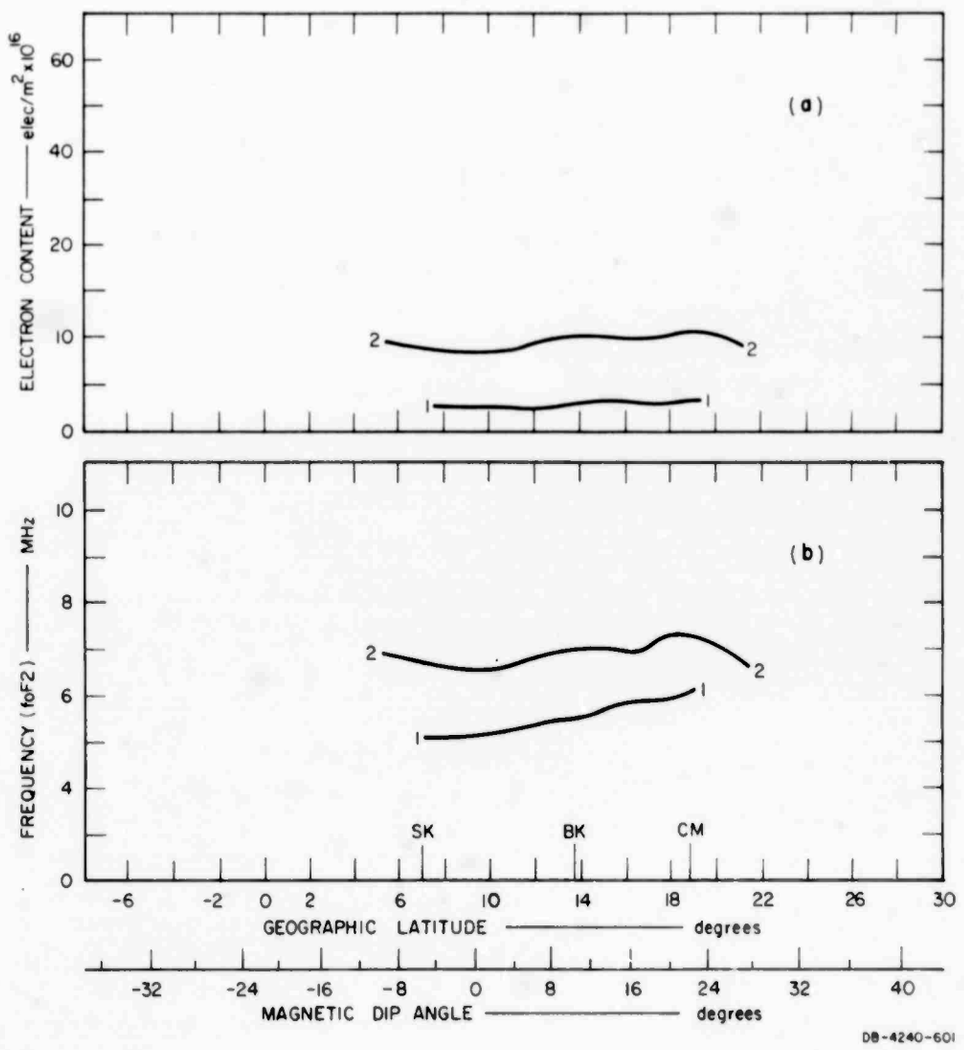

FIG. 12 LATITUDINAL VARIATION OF ELECTRON CONTENT AND F-LAYER ORDINARY CRITICAL FREQUENCY, 0000-0100 LOCAL TIME

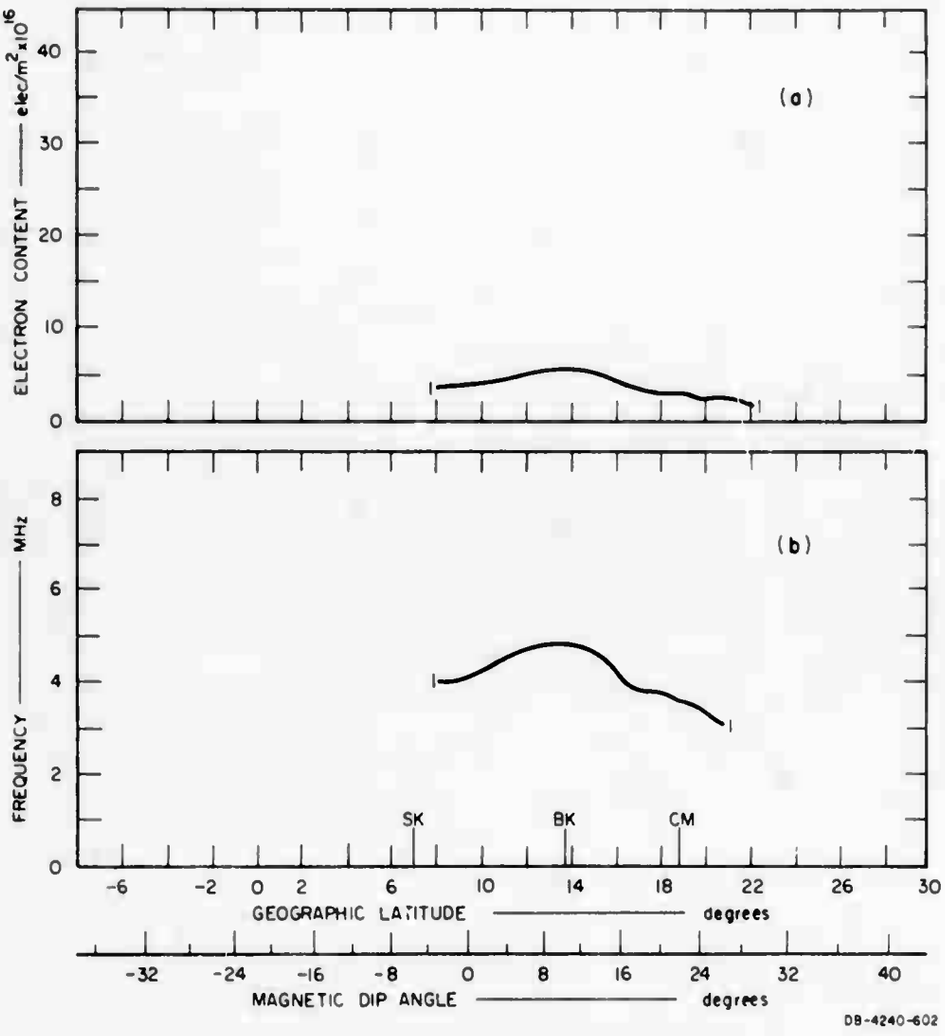

FIG. 13 LATITUDINAL VARIATION OF ELECTRON CONTENT AND F-LAYER ORDINARY CRITICAL FREQUENCY, 0100-0200 LOCAL TIME

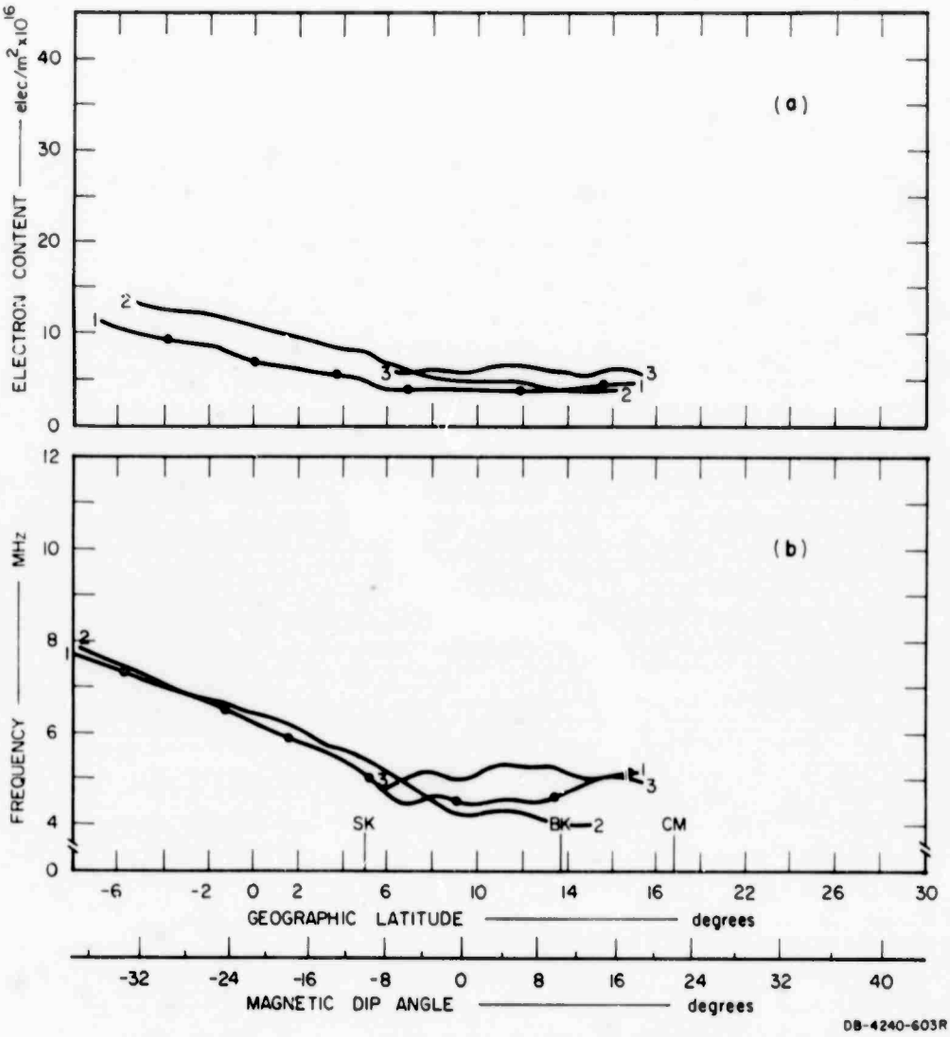

FIG. 14 LATITUDINAL VARIATION OF ELECTRON CONTENT AND F-LAYER ORDINARY CRITICAL FREQUENCY, 0200-0300 LOCAL TIME

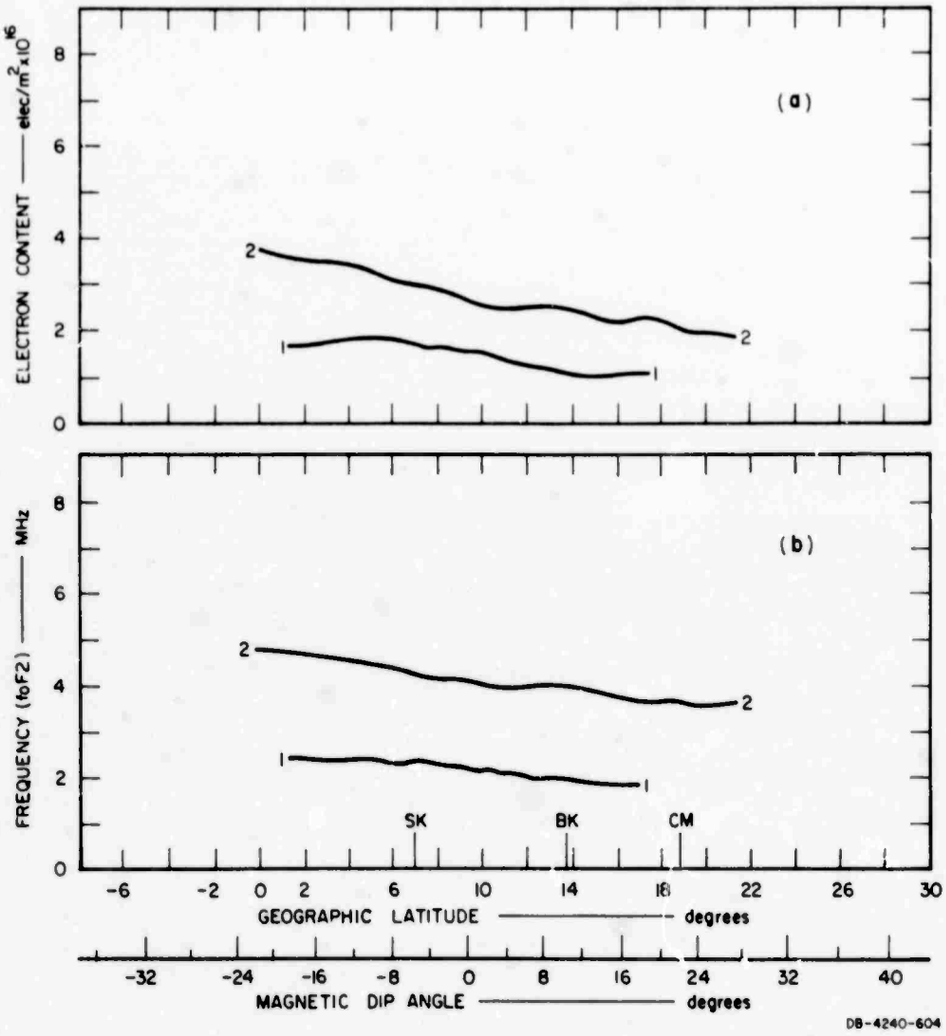

FIG. 15 LATITUDINAL VARIATION OF ELECTRON CONTENT AND F-LAYER ORDINARY CRITICAL FREQUENCY, 0400-0500 LOCAL TIME

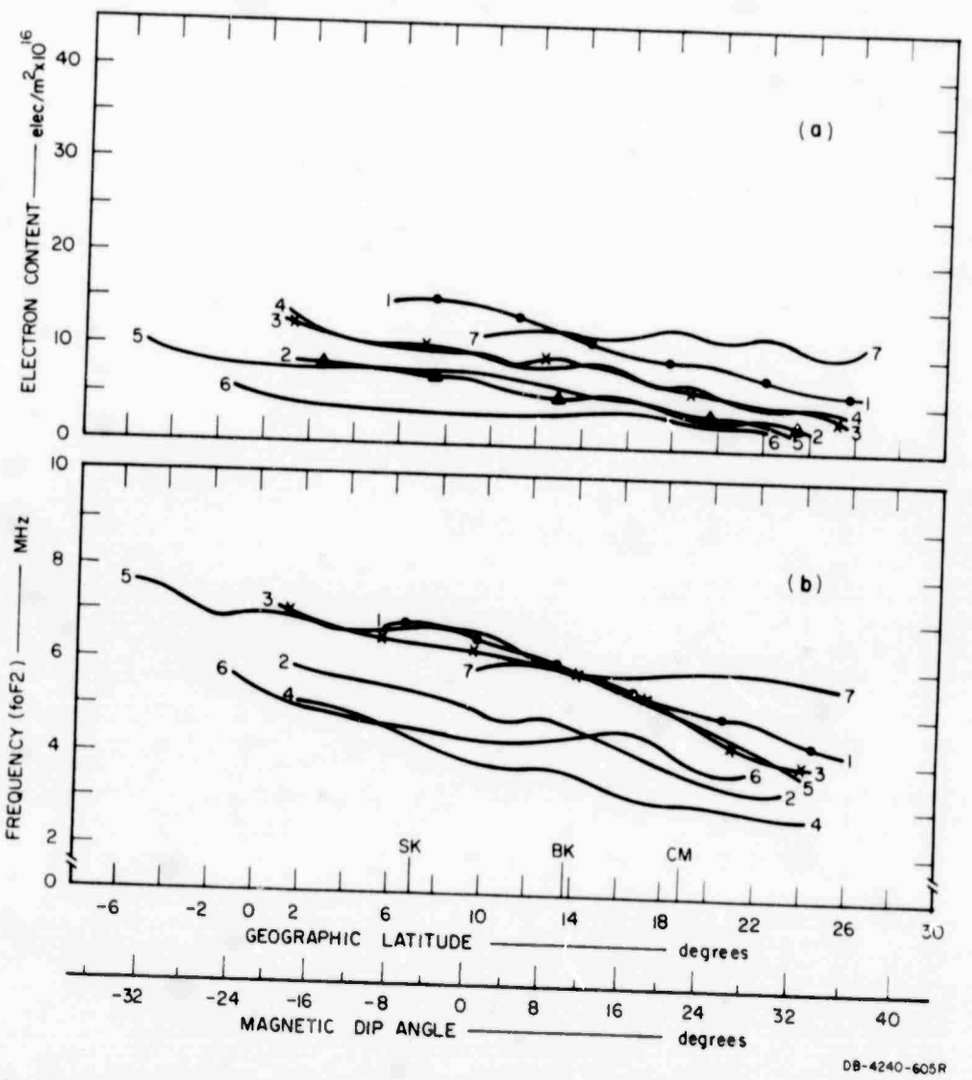

FIG. 16 LATITUDINAL VARIATION OF ELECTRON CONTENT AND F-LAYER ORDINARY CRITICAL FREQUENCY, 0600-0700 LOCAL TIME

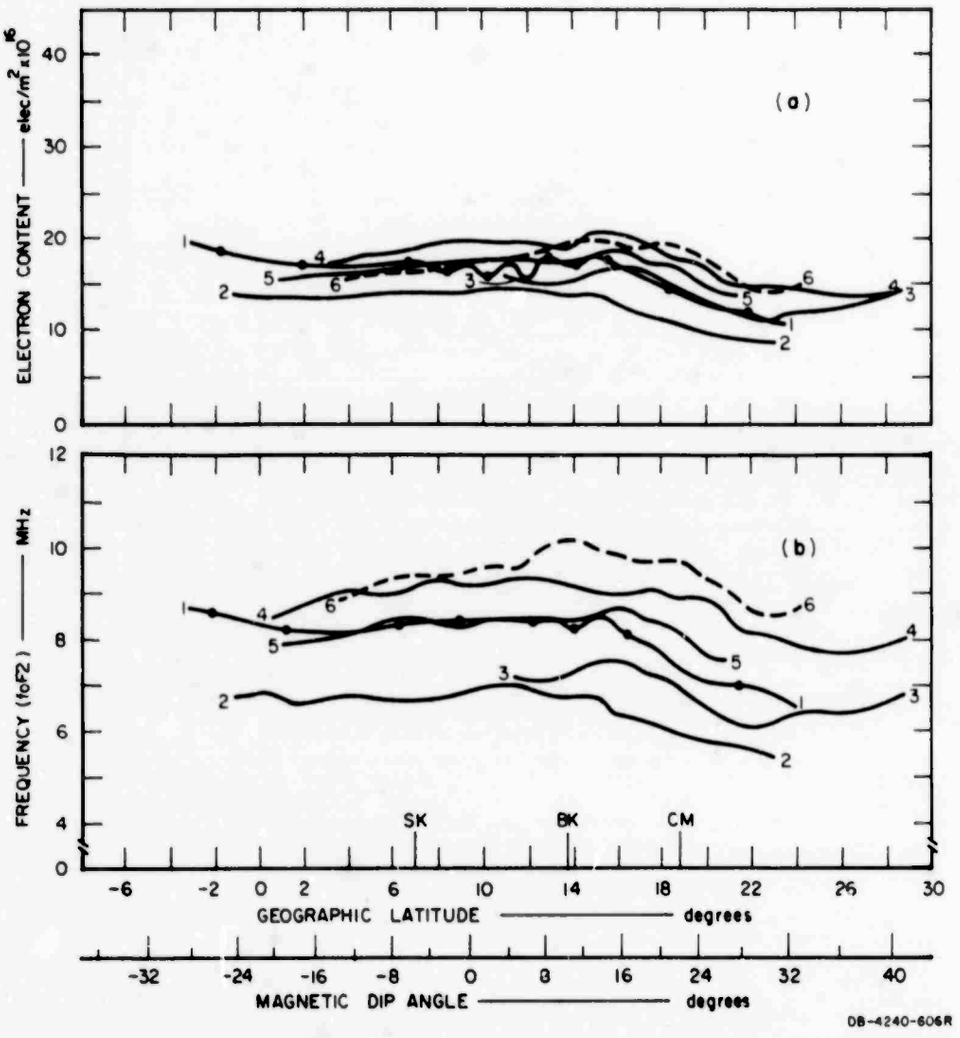

FIG. 17 LATITUDINAL VARIATION OF ELECTRON CONTENT AND F-LAYER ORDINARY CRITICAL FREQUENCY, 0700-0800 LOCAL TIME

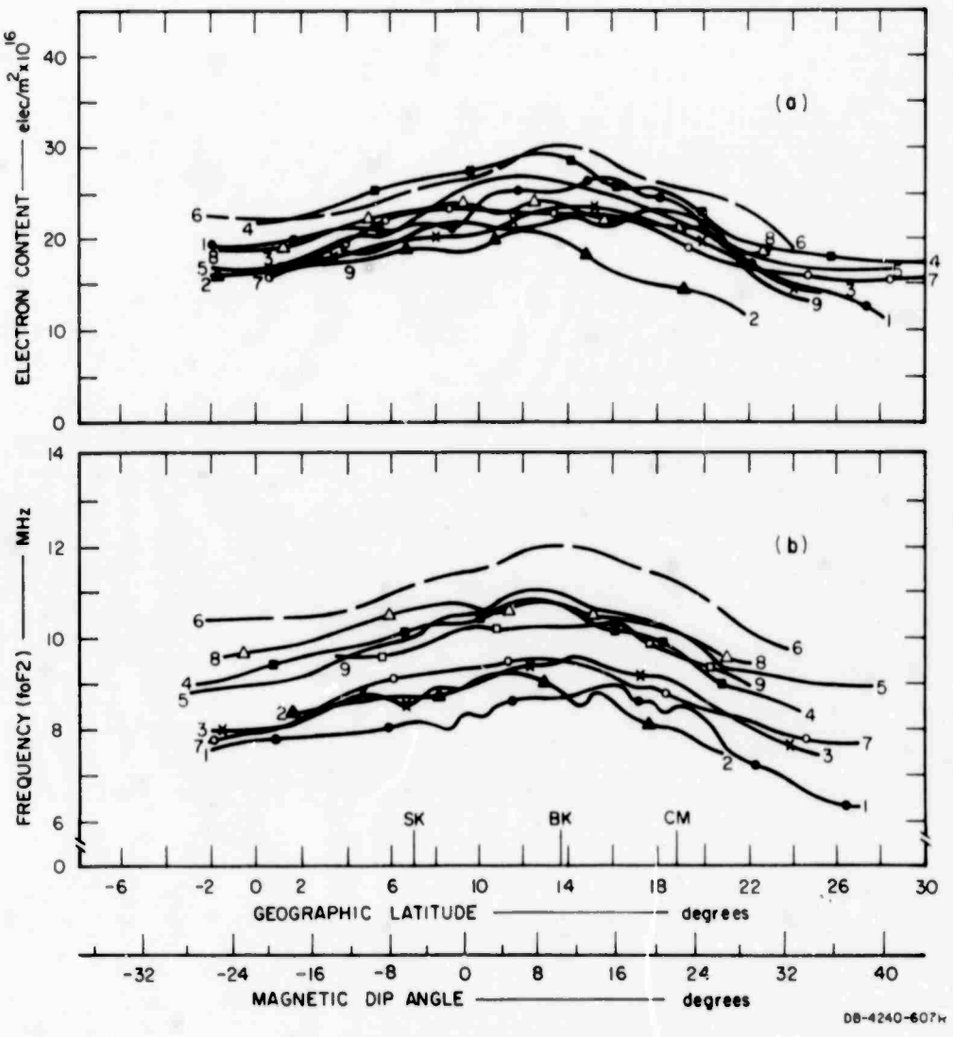

FIG. 18 LATITUDINAL VARIATION OF ELECTRON CONTENT AND F-LAYER ORDINARY CRITICAL FREQUENCY, 0800-0900 LOCAL TIME

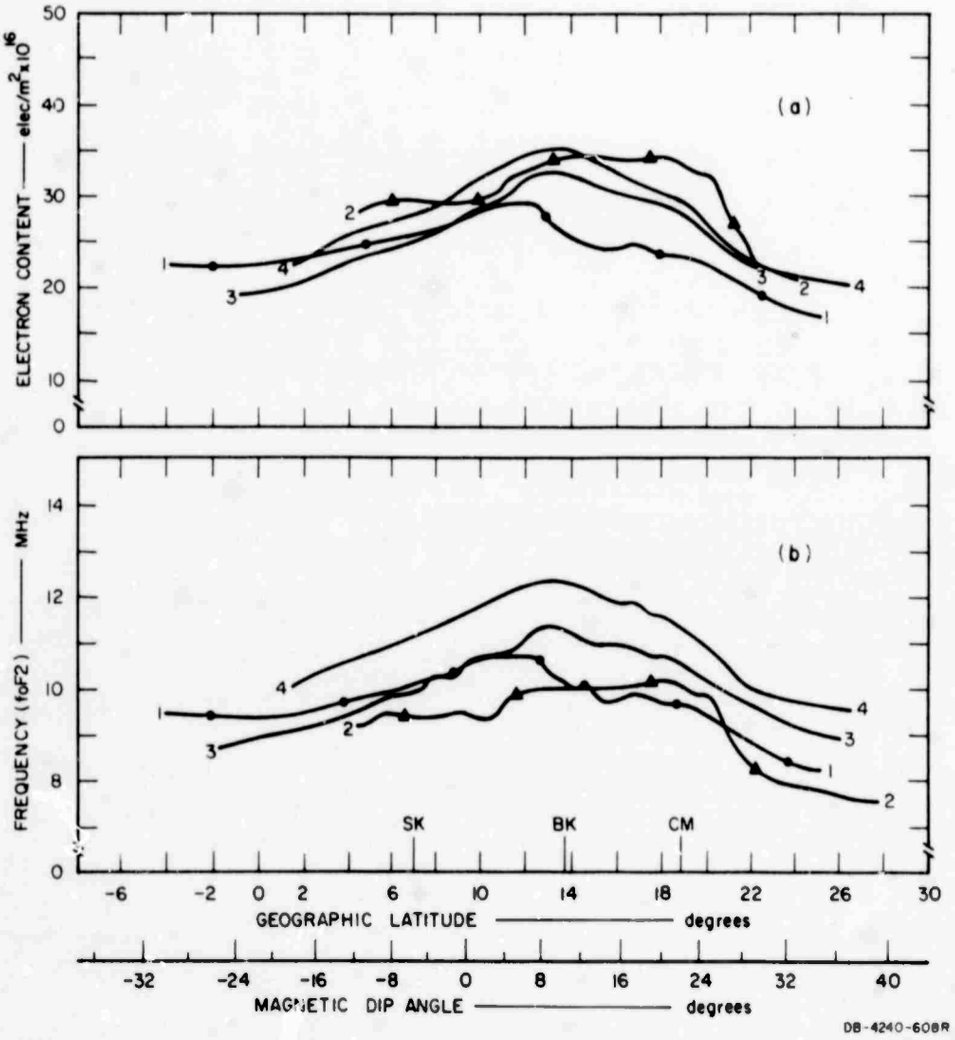

FIG. 19 LATITUDINAL VARIATION OF ELECTRON CONTENT AND F-LAYER ORDINARY CRITICAL FREQUENCY, 0900-1000 LOCAL TIME

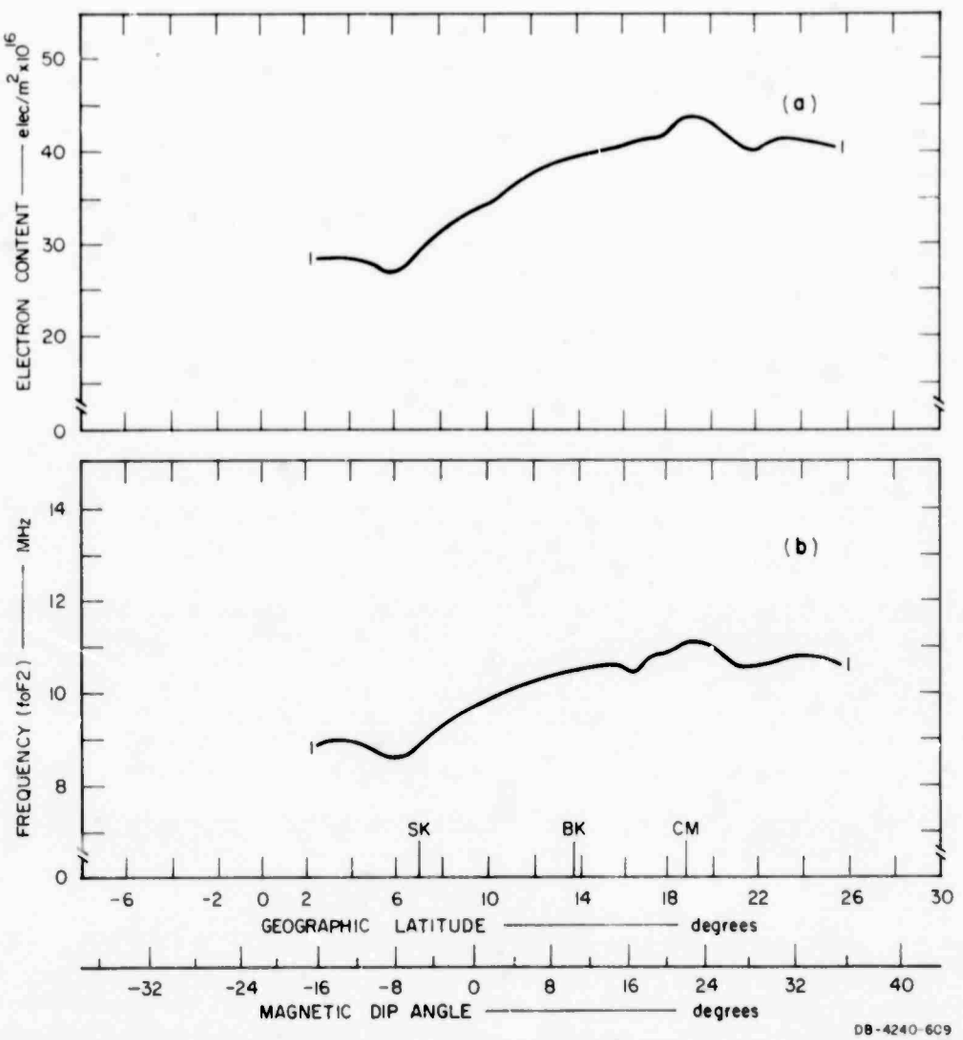

FIG. 20 LATITUDINAL VARIATION OF ELECTRON CONTENT AND F-LAYER ORDINARY CRITICAL FREQUENCY, 1000-1100 LOCAL TIME

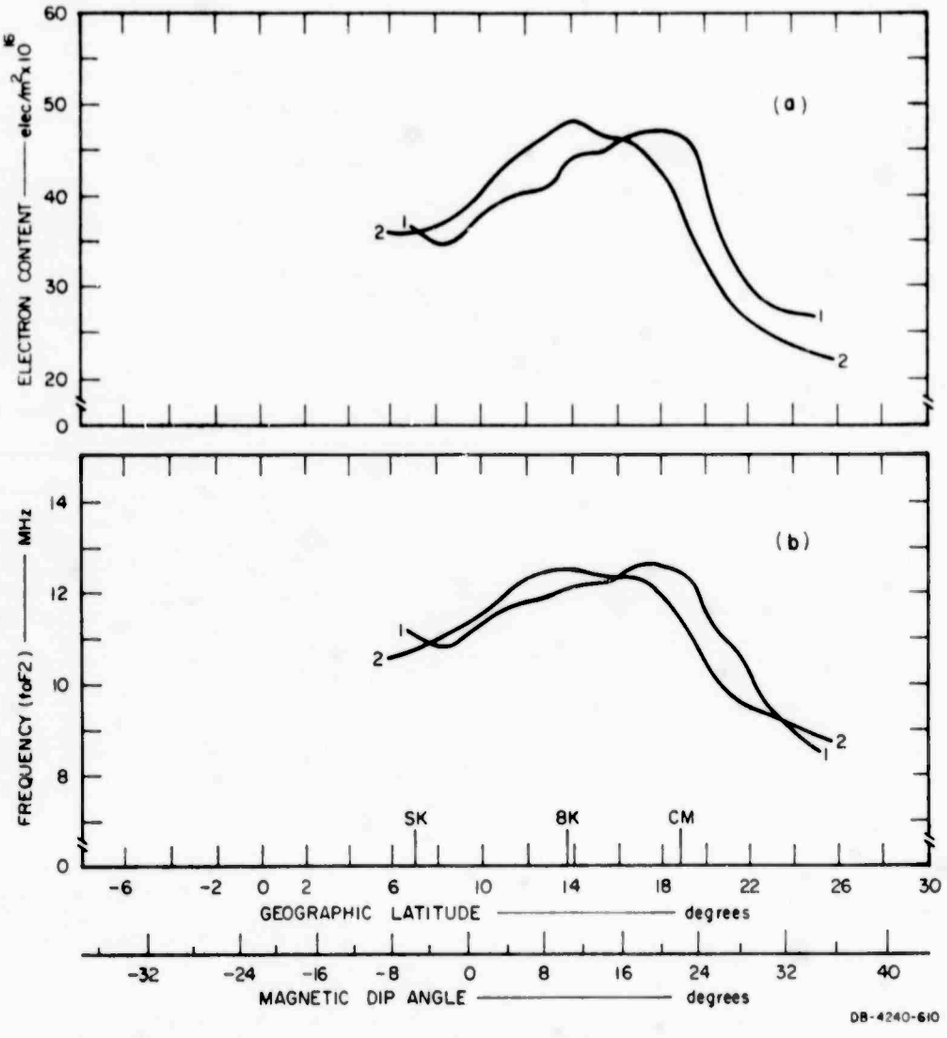

FIG. 21 LATITUDINAL VARIATION OF ELECTRON CONTENT AND F-LAYER ORDINARY CRITICAL FREQUENCY, 1100-1200 LOCAL TIME

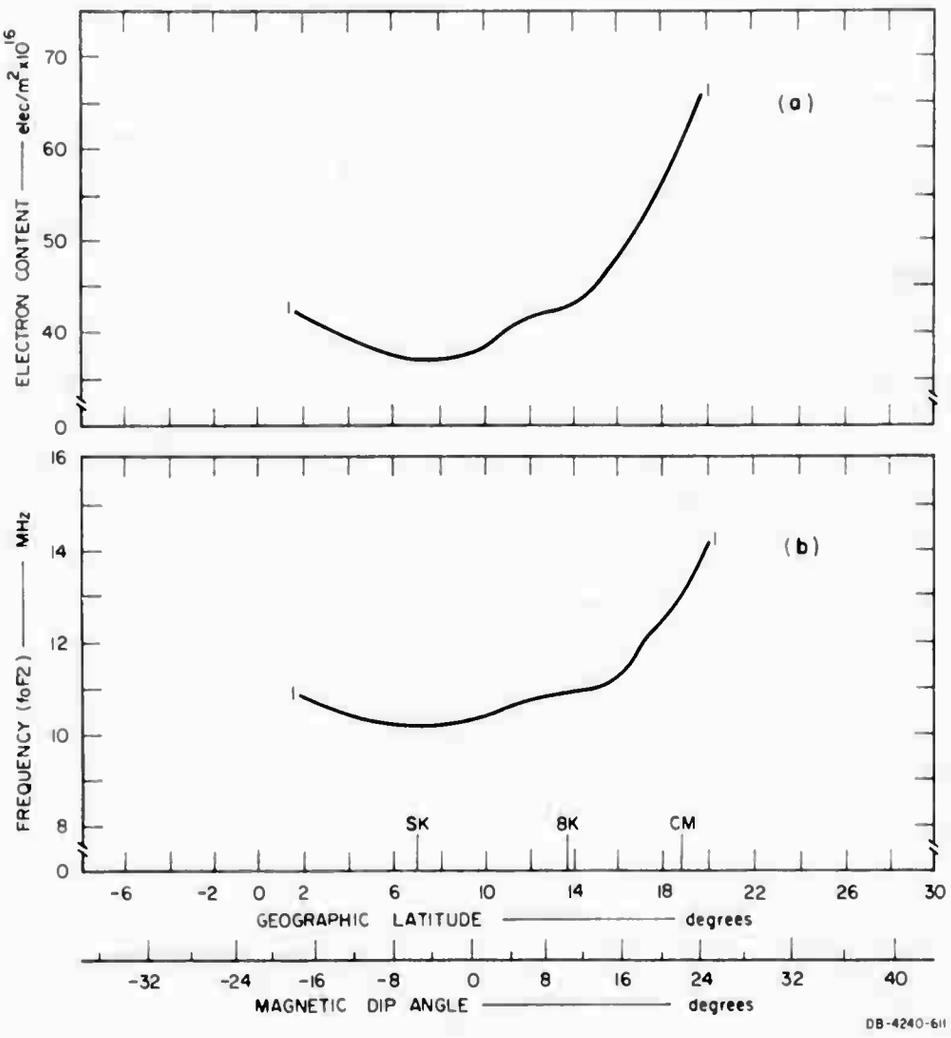

FIG. 22 LATITUDINAL VARIATION OF ELECTRON CONTENT AND F-LAYER ORDINARY CRITICAL FREQUENCY, 1200-1300 LOCAL TIME

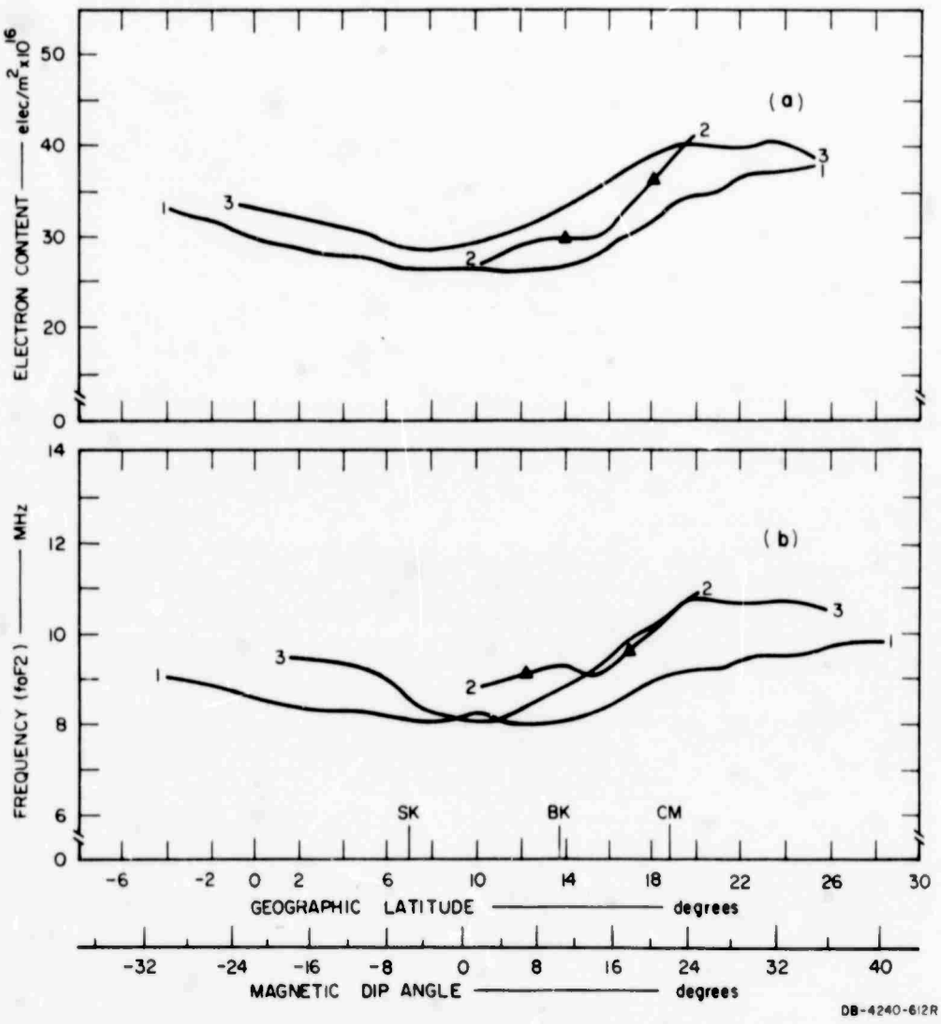

FIG. 23 LATITUDINAL VARIATION OF ELECTRON CONTENT AND F-LAYER ORDINARY CRITICAL FREQUENCY, 1300-1400 LOCAL TIME

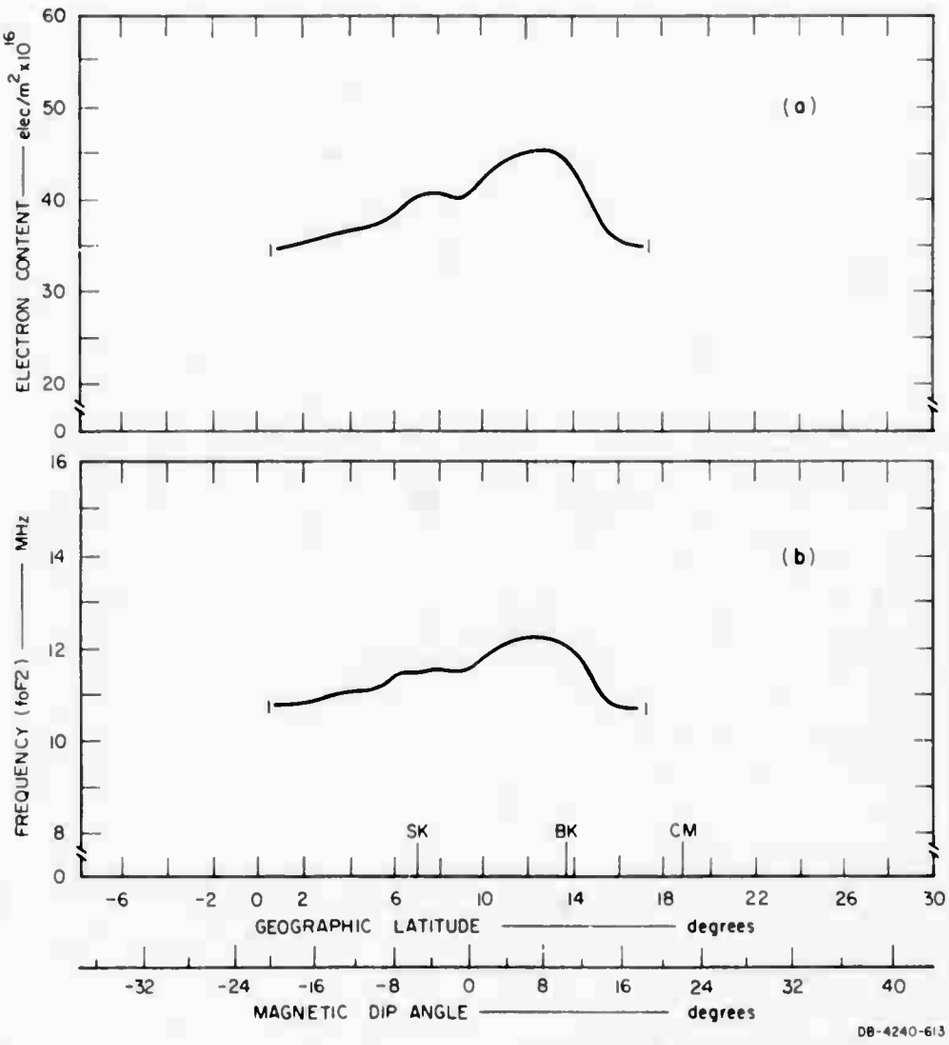

FIG. 24 LATITUDINAL VARIATION OF ELECTRON CONTENT AND F-LAYER ORDINARY CRITICAL FREQUENCY, 1400-1500 LOCAL TIME

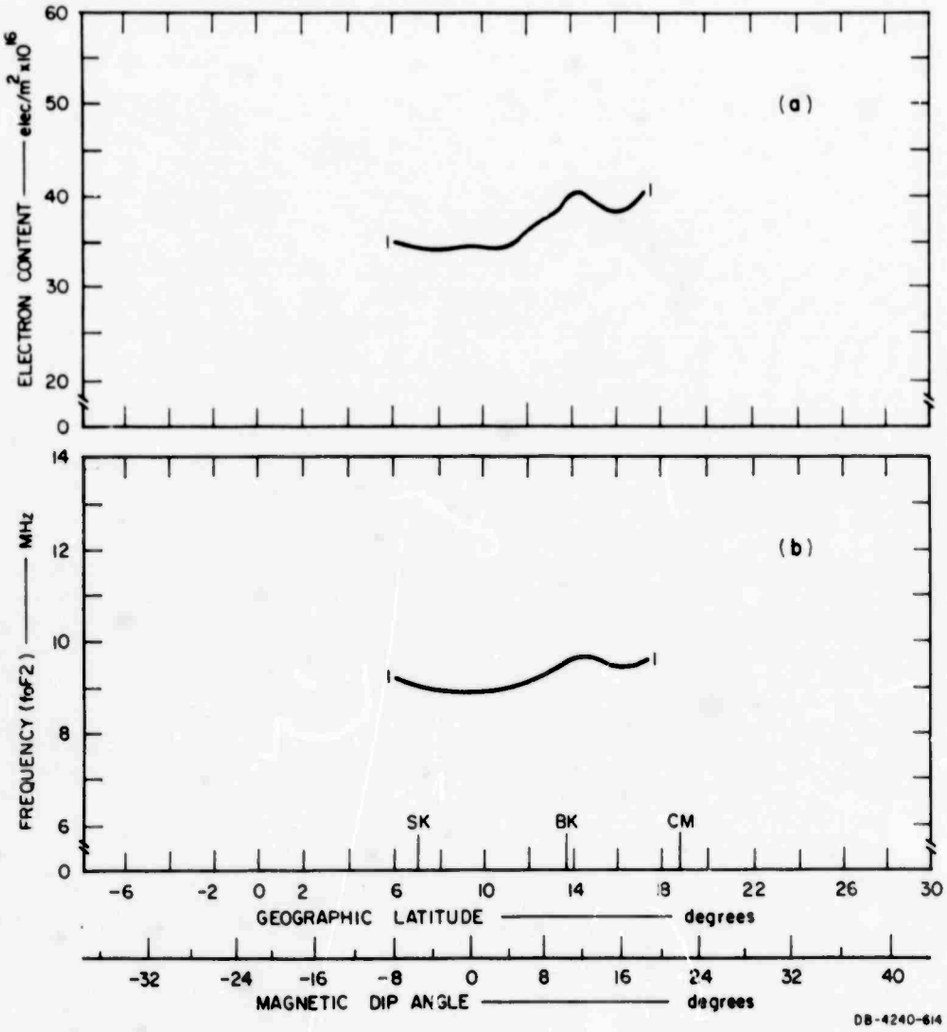

FIG. 25 LATITUDINAL VARIATION OF ELECTRON CONTENT AND F-LAYER ORDINARY CRITICAL FREQUENCY, 1500-1600 LOCAL TIME

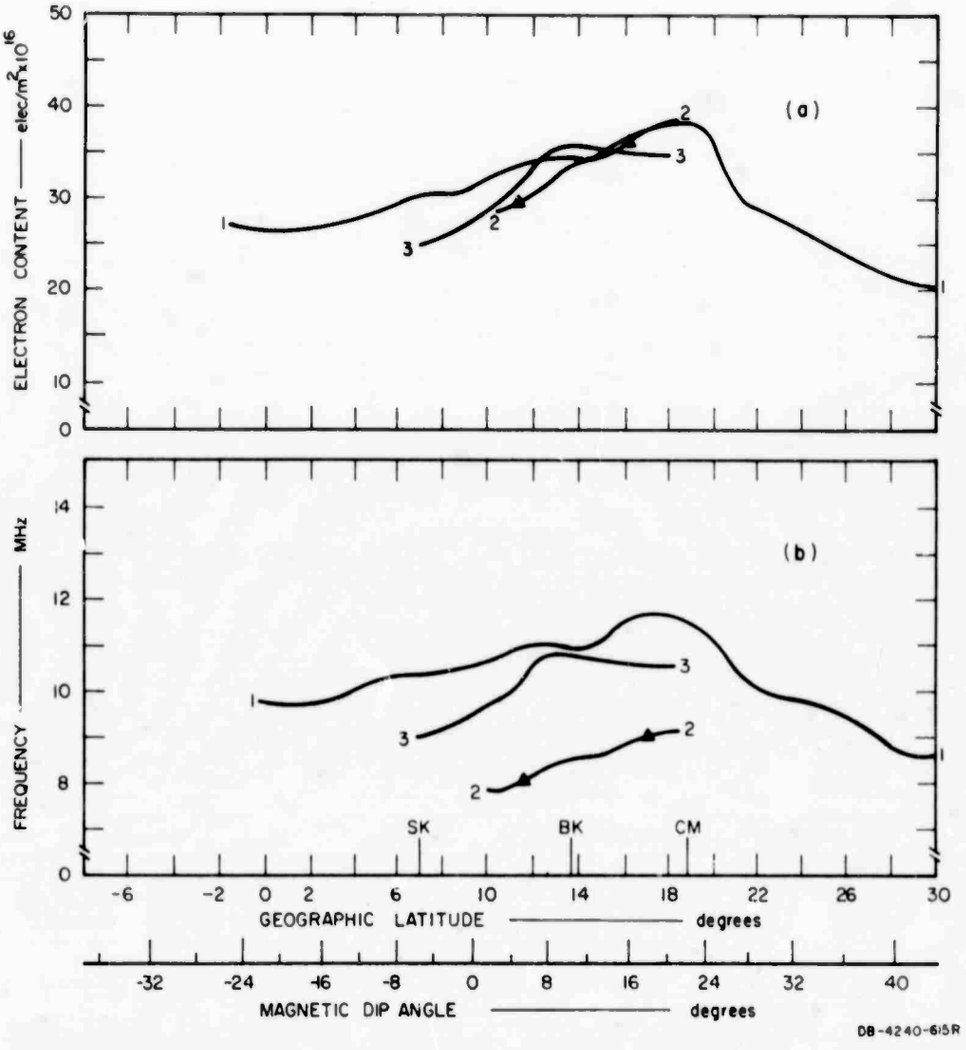

FIG. 26 LATITUDINAL VARIATION OF ELECTRON CONTENT AND F-LAYER ORDINARY CRITICAL FREQUENCY, 1600-1700 LOCAL TIME

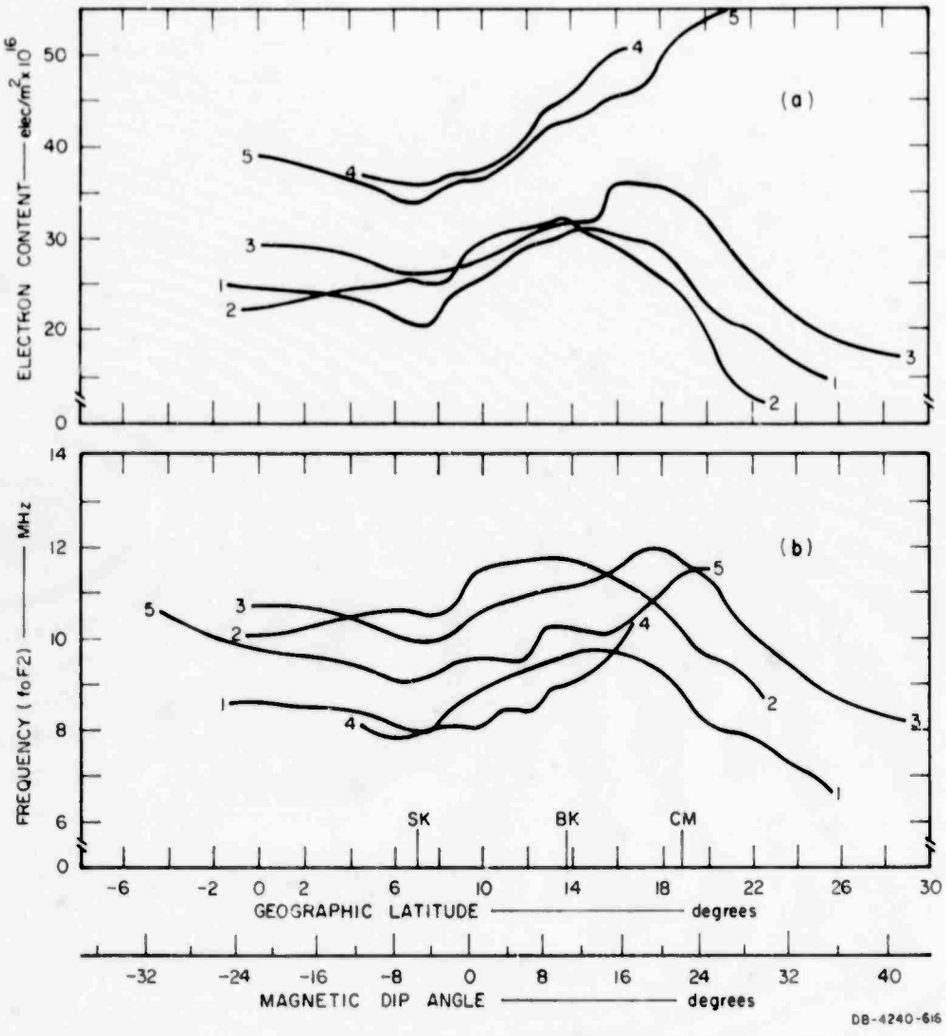

FIG. 27 LATITUDINAL VARIATION OF ELECTRON CONTENT AND F-LAYER ORDINARY CRITICAL FREQUENCY, 1800-1900 LOCAL TIME

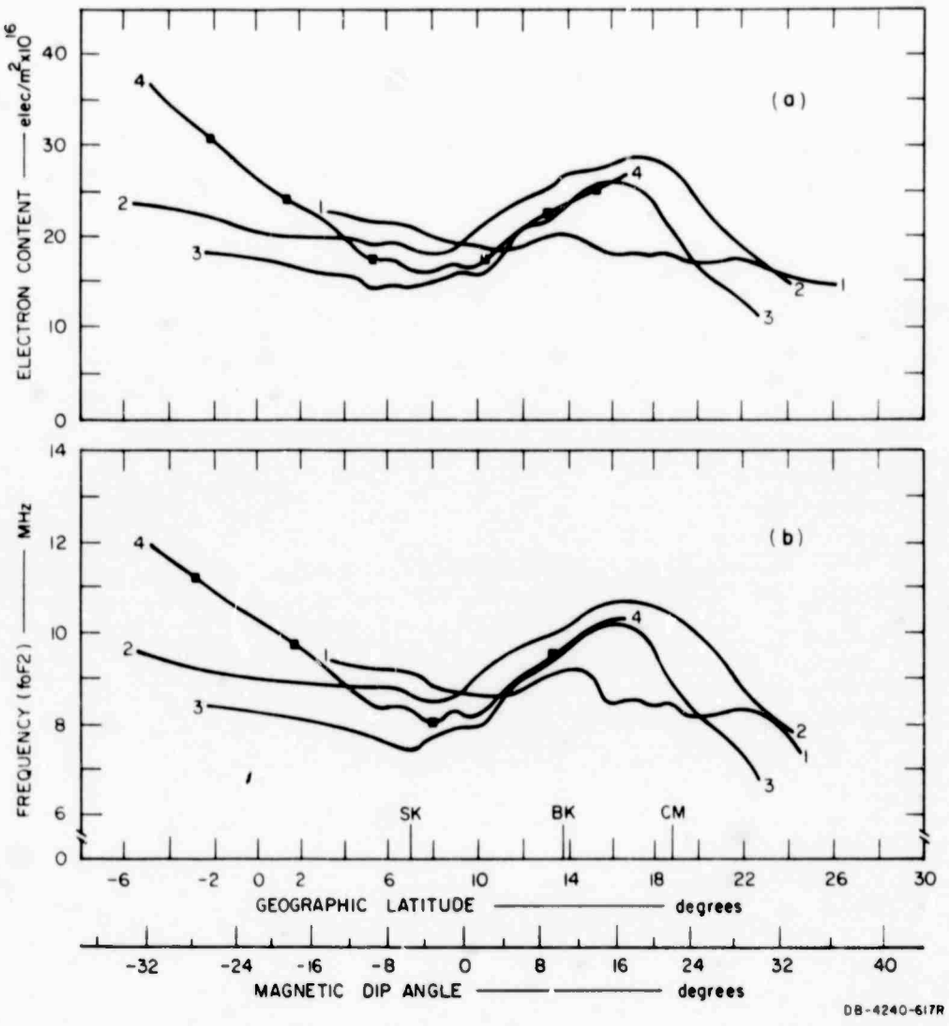

FIG. 28 LATITUDINAL VARIATION OF ELECTRON CONTENT AND F-LAYER ORDINARY CRITICAL FREQUENCY, 1900-2000 LOCAL TIME

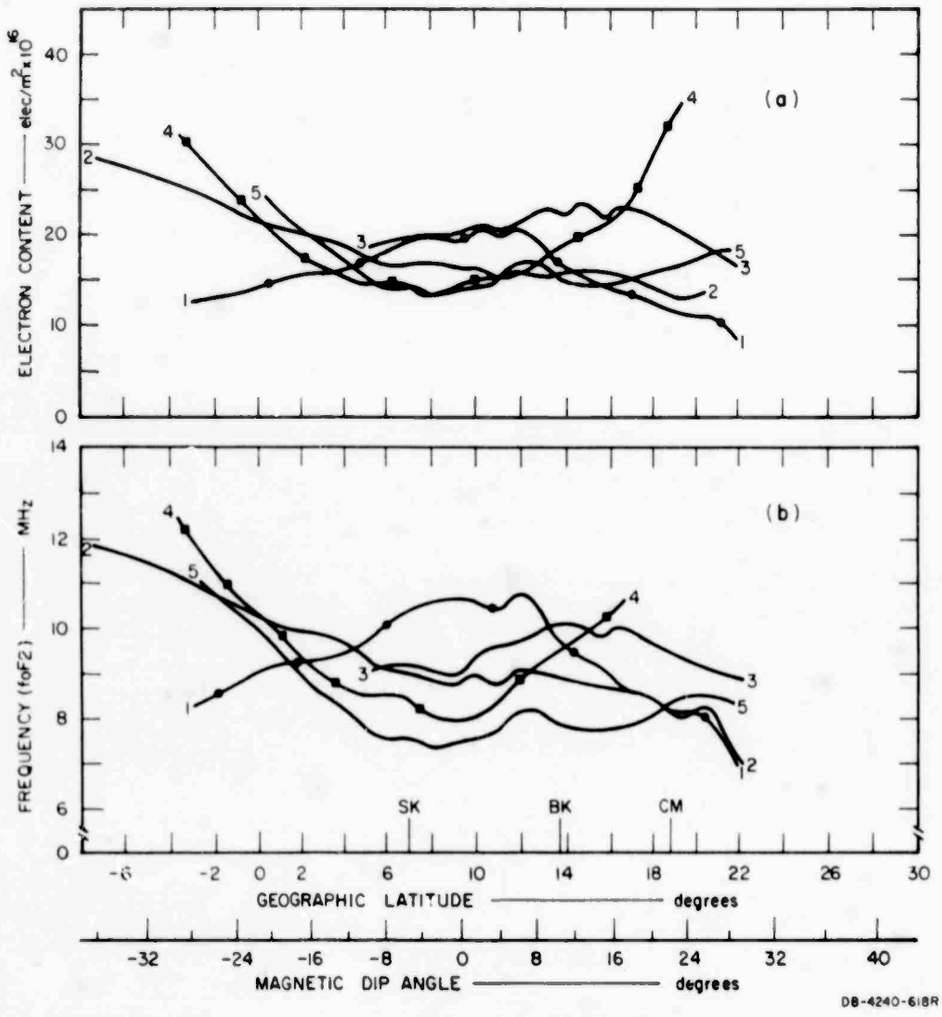

FIG. 29 LATITUDINAL VARIATION OF ELECTRON CONTENT AND F-LAYER ORDINARY CRITICAL FREQUENCY, 2000-2100 LOCAL TIME

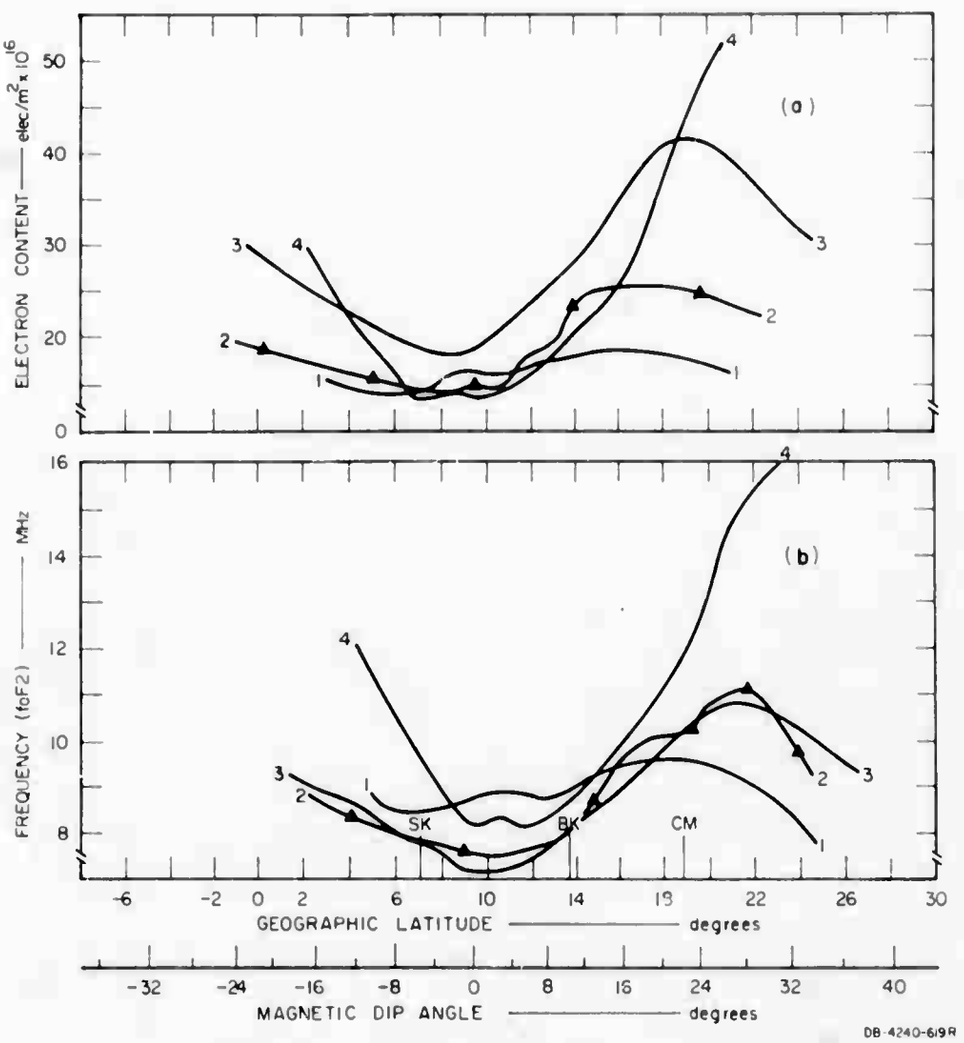

FIG. 30 LATITUDINAL VARIATION OF ELECTRON CONTENT AND F-LAYER ORDINARY CRITICAL FREQUENCY, 2100-2200 LOCAL TIME

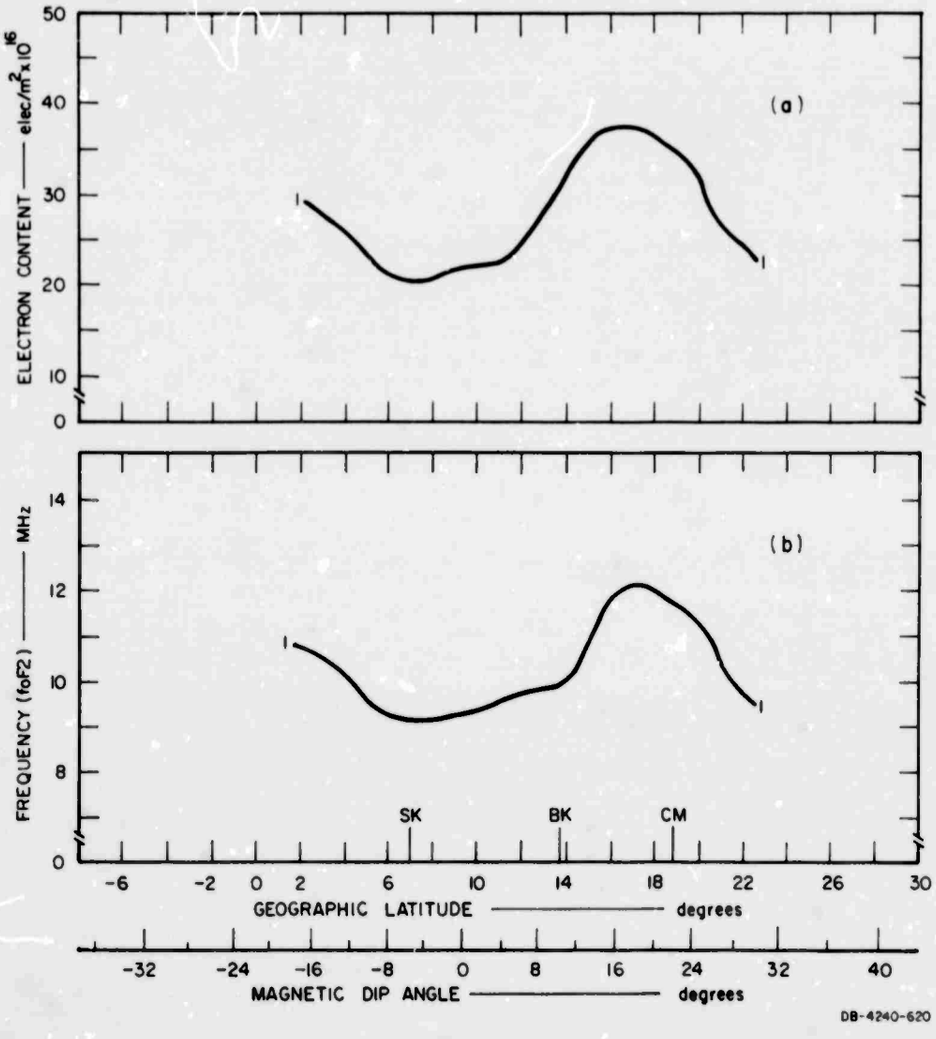

FIG. 31 LATITUDINAL VARIATION OF ELECTRON CONTENT AND F-LAYER ORDINARY CRITICAL FREQUENCY, 2200-2300 LOCAL TIME

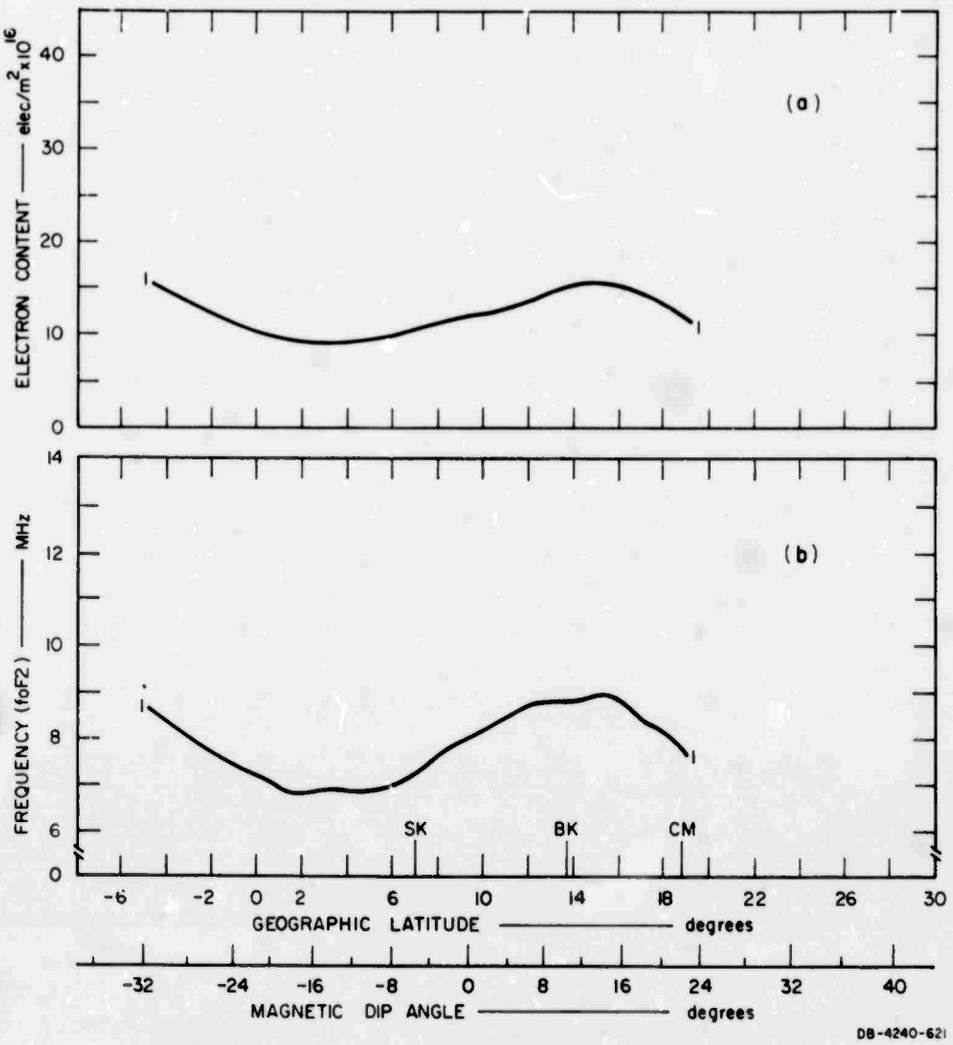

FIG. 32 LATITUDINAL VARIATION OF ELECTRON CONTENT AND F-LAYER ORDINARY CRITICAL FREQUENCY, 2300-0000 LOCAL TIME

B. LATITUDINAL VARIATION OF F-LAYER CRITICAL FREQUENCY

Data collected for calculating electron content of the ionosphere by the Faraday rotation measurements can be used to estimate the latitudinal variation of the F-layer ordinary-wave critical frequency, foF2. There have been many attempts to show that the model ionosphere used for calculation of the total electron content is not too critical--except for the refraction correction.[17-20] To determine the latitudinal variation of the F-layer ordinary critical frequency, Chapman's equation was chosen to represent the electron density distribution with height of the ionosphere. Although several very questionable assumptions were made by Chapman in the derivation of his formula, the general shape of the electron density distribution with altitude as given by Chapman's equation still gives a reasonable fit to the actual distribution profile as we know it.[6,16,20,21] A simple equation has been proposed by Wright[22] and Potts[14] for the ionospheric electron-density distribution profile. This equation assumed that the shape of the profile was similar to that given by Chapman's equation and the F-layer ordinary wave frequency (foF2), and can be expressed in terms of total electron content and mean scale height as

$$foF2 = \left[\frac{\int Ndh}{5.12\ \bar{H} \times 10^{10}}\right]^{\frac{1}{2}} \quad . \qquad (17)$$

Substituting Eq. (9) into Eq. (17) gives

$$foF2 = \left[\frac{R}{5.12\ \bar{GH} \times 10^{10}}\right]^{\frac{1}{2}} \quad . \qquad (18)$$

The method for calculating foF2 as a function of latitude is very similar to the method for calculating values of latitudinal electron content. A computer program has been prepared for the computation of the latitudinal variations of foF2 values. In this study, the value of mean scale height ($\bar{H}$) was taken from the data of Fig. 10, which includes the diurnal variation of $\bar{H}$ at Bangkok derived by the rotation-rate method of Faraday analysis. The value of mean scale height in the F region of the ionospheric profile was assumed to be constant in latitude for the equatorial region. Allowing this present assumption, the

similarity between the theoretical and experimental values of mean scale height have been reported.[20,23,24]

The calculated values of foF2 are computed from the same selected Faraday fading records that were used for the analysis of latitudinal variation of total electron content. The results are shown in Part (b) of Figs. 12 through 32. The calculated values are for the points on the sub-ionospheric path in the shaded zones of Fig. 11. The latitudinal variations of foF2 showed diurnal development and collapse of the equatorial anomaly. This anomaly shows that the magnetic equator is nearly midway in the latitude range depicted. The results are associated with the diurnal development and collapse of the equatorial anomaly in total electron content value, and illustrate the similarity between electron content and foF2. The results are represented in a schematic illustration in Fig. 33, which shows in simplified form the diurnal development and collapse of the equatorial anomalies of foF2 value for the winter solstice. During the period 0000-0700 local time the latitude variation of foF2 is rather linear, with the southern-most foF2 values significantly higher, as illustrated in Part (a) of Fig. 33. The latitudinal variation of foF2 is characterized by a peak near the magnetic equator during the period 0700-1000 local time, as illustrated in Part (b) of Fig. 33. The well-defined development of the equatorial anomaly occurred during the period 1000-1600 local time. The trough near the magnetic equator during this time is illustrated in Part (c) of Fig. 33. The equatorial trough anomaly collapsed during the next interval. Next, a peak formed and shifted north of the magnetic equator near the sunset hour 1700-1800 local time, as illustrated in Part (d). The equatorial trough anomaly is developed again during the period 1800-0000 local time, as illustrated in Part (e) of Fig. 33.

To check the validity of the latitudinal variation of foF2 as deduced from the Faraday rotation data, the results were compared with data from vertical-incidence sounders taken at times corresponding to satellite passages. The observed foF2 values at Chiengmai and Songkhla are obtained from Granger sounders which were operated at these field sites while the Faraday measurements were made. Due to the lower frequency

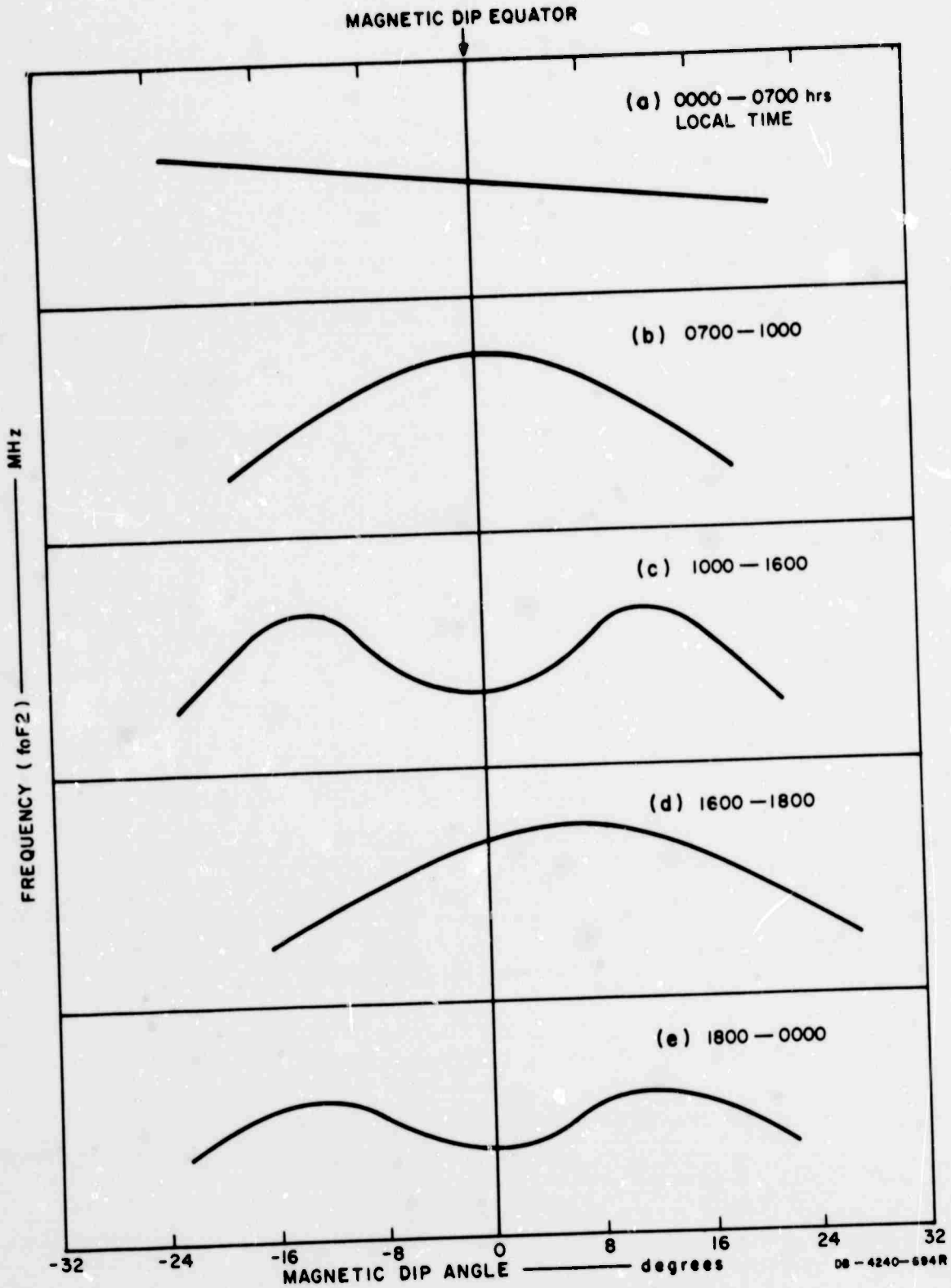

FIG. 33 SCHEMATIC ILLUSTRATION OF THE DEVELOPMENT AND COLLAPSE OF EQUATORIAL ANOMALIES

limit of these sounders, frequencies below 4 MHz are not available for comparison. A comparison of the calculated and observed values for these three stations operating ionosondes is presented in Appendix D. The calculated values are for the points on the sub-ionospheric path nearest the ionosonde locations. The results compare well with the observed values. The typical difference observed is less than 10 percent.

VI SUMMARY AND CONCLUSIONS

This report presents the experimental observations of the equatorial ionosphere made from Faraday rotation measurements. Diurnal variations of electron content over Bangkok show low early-morning values, and maximum values in the afternoon. Typically, the total electron content varied from 1×10^{16} electrons/m^2 to 55×10^{16} electrons/m^2. The seasonal variations show the maximum values of electron content occurring near the equinoctial periods and minimum values occurring near the solstitial periods.

The results of the latitudinal variations of electron content and foF2 show the diurnal development and collapse of the equatorial anomalies. The results show similarity between electron content and foF2. During the period 0000-0700 local time, the anomaly in latitudinal variation is rather flat. It is characterized by a peak near the magnetic equator during the period 0700-1000 local time. A well-defined development of the equatorial anomaly occurs during the period 1000-1600 local time, exhibiting a trough near the magnetic equator. The equatorial anomaly collapses to a peak and shifts north of the magnetic equator near the sunset hour 1700-1800 local time; the equatorial-trough anomaly develops again during the period 1800-0000 local time.

The experimental results of foF2 from Faraday rotation data have been compared with ionosonde data, usually with agreement within 10 percent. The latitudinal variation of foF2 shows the diurnal development and collapse of the equatorial anomaly. The scan of foF2 as a function of latitude can be used to adjust the foF2 observed by the C-2 ionosonde at Bangkok for the prediction of maximum useful frequency (MUF) in other parts of Thailand. These adjustments are needed because, when the largest gradients occur (between the development and collapse conditions of the equatorial anomalies), the variation can significantly affect the MUF of HF radio systems in Thailand. It has been shown that observed foF2 for Bangkok, when available, can be used to improve local

frequency prediction.[25,28] The latitudinal variations of foF2 value presented provide information permitting improved predictions of MUF for areas in Thailand where ionosonde data are not available.

Appendix A

DERIVATION OF THE GEOMETRICAL COEFFICIENT G-VALUES

Appendix A

DERIVATION OF THE GEOMETRICAL COEFFICIENT G-VALUE

The method of calculation of the G-value is given in this appendix in detail, for the purpose of providing a computer program for direct application to the analysis of the Faraday rotation data from satellite radio signals.

The G value is calculated at an ionospheric centroid height and evaluating the magnetic field at that altitude. Assume no refraction in the ionosphere or lower atmosphere. Consider the geometry shown in Figs. A-1 and A-2, where the coordinates of the subsatellite point A

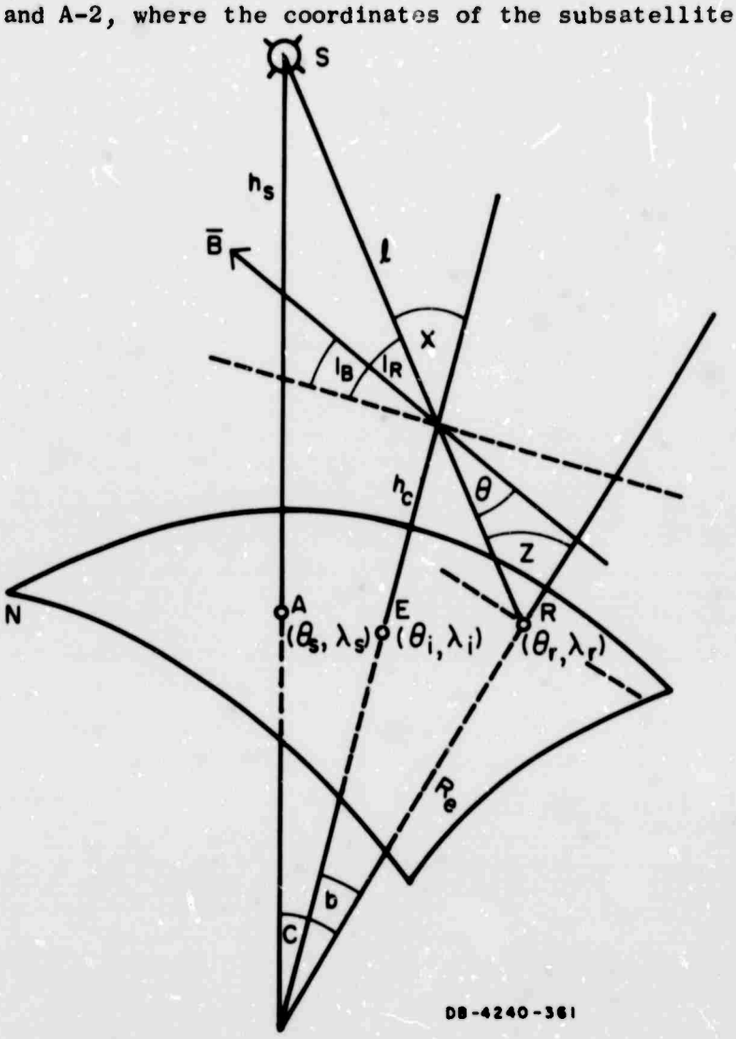

FIG. A-1 GEOMAGNETIC--FIELD/RAY-PATH GEOMETRY

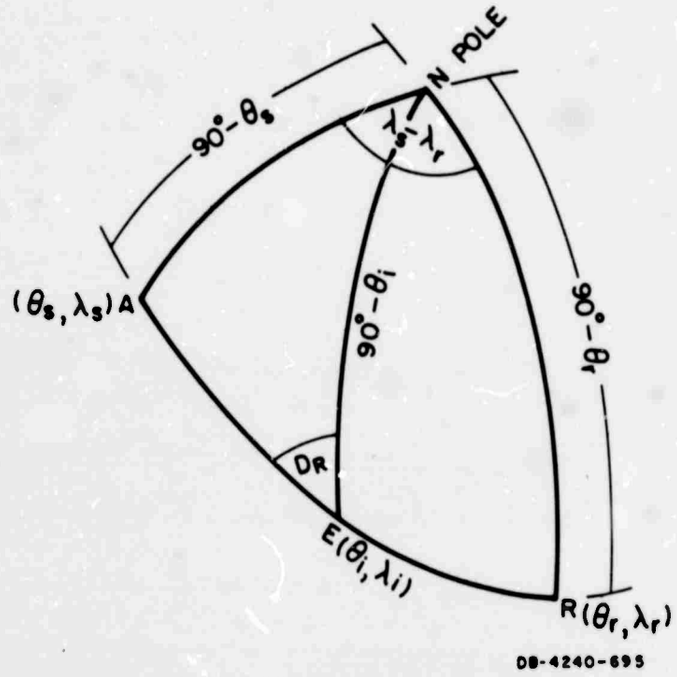

FIG. A-2 SURFACE ARC DISTANCE

(the projection of satellite on the earth), the subsatellite point E (the projection on the earth of the intersection of the ray path between satellite and ground station, with the centroid of the ionospheric electron density profile), and the ground station, R, are θ_s, λ_s; θ_i, λ_i; and θ_r, λ_r; geographic latitude and longitude, respectively. The earth's radius is denoted by R_e and the ionospheric centroid height is h_c. Satellite height is h_s.

By using spherical trigonometry, the angular range C (measured at the center of the earth) is:

$$\cos C = \sin \theta_s \sin \theta_r + \cos \theta_s \cos \theta_r \cos (\lambda_s - \lambda_r) . \qquad \text{(A-1)}$$

Let the slant distance from satellite to ground station be equal to ℓ:

$$\ell = [R_e^2 + (R_e + h_s)^2 - 2R_e(R_e + h_s) \cos C]^{\frac{1}{2}} . \qquad \text{(A-2)}$$

The inclination of signal ray, I_R, and satellite zenith angle, χ, at the ionospheric centroid height can be determined as

$$I_R = \cot^{-1}\left[\frac{R_e\,(R_e + h_s)\,\sin C}{\left\{(R_e+h_c)^2\,[R_e^2+(R_e+h_s)^2-2R_e(R_e+h_s)\cos C] - [R_e(R_e+h_s)\sin C]^2\right\}^{1/2}}\right] \tag{A-3}$$

$$\chi = 90^\circ - I_R \tag{A-4}$$

$$\sec \chi = \operatorname{cosec} I_R \,. \tag{A-5}$$

The observing satellite zenith angle, Z, is

$$Z = 90^\circ - \cos^{-1}\left[\frac{R_e + h_c}{R_e}\ \sin \chi\right] . \tag{A-6}$$

Figure A-2 shows the arcs of the earth's surface from the geographical north pole to the subsatellite point, subionospheric, point and ground stations. (If more convenient, we may join them to the geographical south pole.) Then the subionospheric point E (θ_i, λ_i) is

$$\theta_i = \sin^{-1}\ [\sin \theta_r\ (\cos b - \sin b \cot C) + \sin \theta_s \sin b \operatorname{cosec} C] \tag{A-7}$$

$$\lambda_i = \lambda_r + N \qquad (\text{If } \lambda_s \geq \lambda_r) \tag{A-8}$$

$$\lambda_i = \lambda_r - N \qquad (\text{If } \lambda_s \leq \lambda_i) \tag{A-9}$$

where

$$N = \sin^{-1}\left\{\frac{\sin b}{\cos \theta_i}\left[1 - \left(\frac{\sin \theta_s - \sin \theta_r \cos C}{\cos \theta_r \sin C}\right)^2\right]^{1/2}\right\} \tag{A-10}$$

and

$$b = \cos^{-1}\left[\frac{R_e(R_e + h_s)\,\sin C}{(R_e + h_c)[R_e^2 + (R_e + h_s)^2 - 2R_e(R_e + h_s)\cos C]^{1/2}}\right]$$

$$-\cos^{-1}\left[\frac{(R_e + h_s)\,\sin C}{[R_e^2 + (R_e + h_s)^2 - 2R_e(R_e + h_s)\cos C]^{1/2}}\right] \tag{A-11}$$

The declination of the signal ray, D_R, at the ionospheric centroid height can be determined by:

$$D_R = \cos^{-1}\left[\frac{\sin\theta_s}{\cos\theta_i \sin(C - b)} - \tan\theta_i \cot(C - b)\right] . \quad (A\text{-}12)$$

The angle between signal ray path and earth's magnetic field, θ, can be determined by the geometry as shown in Fig. A-3. Let OX, OY, and OZ be three perpendicular lines through the ionospheric centroid height at Point O, where I_B and D_B are magnetic dip angle and declination, respectively. Using the direction cosines theorem, the earth's magnetic field $\overline{OB}$ is in the direction with the direction cosines ($\cos\alpha_B$, $\cos\beta_B$, $\cos\gamma_B$), and the signal ray OS is in the directions ($\cos\alpha_R$, $\cos\beta_R$, $\cos\gamma_R$). By the rule for the addition of direction cosines, the angle, θ, between $\overline{OB}$ and OS can be determined by

$$\cos\theta = \cos\alpha_R \cos\alpha_B + \cos\beta_R \cos\beta_B + \cos\gamma_R \cos\gamma_B . \quad (A\text{-}13)$$

By the spherical trigonometry, we can solve for the cosine value as follows:

$$\cos\alpha_R = \cos I_R \cos D_R$$

$$\cos\beta_R = \cos I_R \sin D_R$$

$$\cos\gamma_R = \sin I_R \quad (A\text{-}14)$$

and

$$\cos\alpha_B = \cos I_B \cos D_B$$

$$\cos\beta_B = \cos I_B \sin D_B$$

$$\cos\gamma_B = \sin I_B . \quad (A\text{-}15)$$

Substituting Eqs. (A-11) and (A-12) into (A-10),

$$\cos\theta = \cos I_R \cos I_B \cos(D_R - D_B) + \sin I_R \sin I_B . \quad (A\text{-}16)$$

Note that I_R, I_B is positive when the direction is below the horizontal. Since Fig. A-1 shows that I_R (direction of signal ray from satellite) is always negative, Eq. (A-14) becomes

$$\cos\theta = \cos I_R \cos I_B \cos(D_R - D_B) - \sin I_R \sin I_B . \quad (A\text{-}17)$$

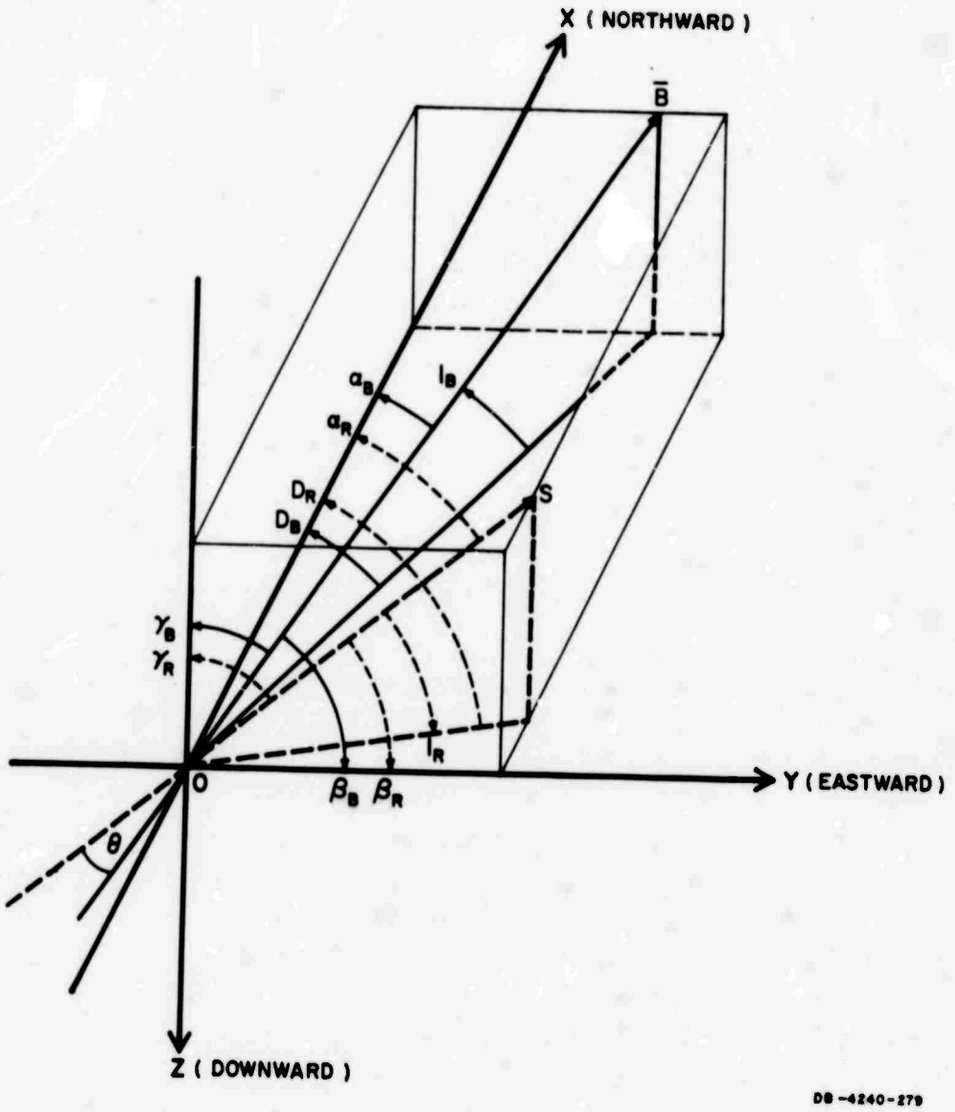

FIG. A-3 RECTANGULAR COORDINATE OF GEOMAGNETIC FIELD/RAY PATH

The value of G can be calculated for any time during the satellite pass for which a measurement of electron content is performed. The expression for the G value from Eqs. (A-5) and (A-17) is then

$$G = B \cos \theta \sec \chi \quad . \tag{A-18}$$

The value of B in Eq. (A-18) is properly specified by the spherical harmonic expansion of the first six harmonics to which about 0.3 percent of the local geomagnetic field measurements during magnetically quiet conditions.[27] The first six harmonics of spherical harmonic expansion are described in detail by the author in Ref. 28.

Appendix B

COMPUTER PROGRAM FLOWCHARTS

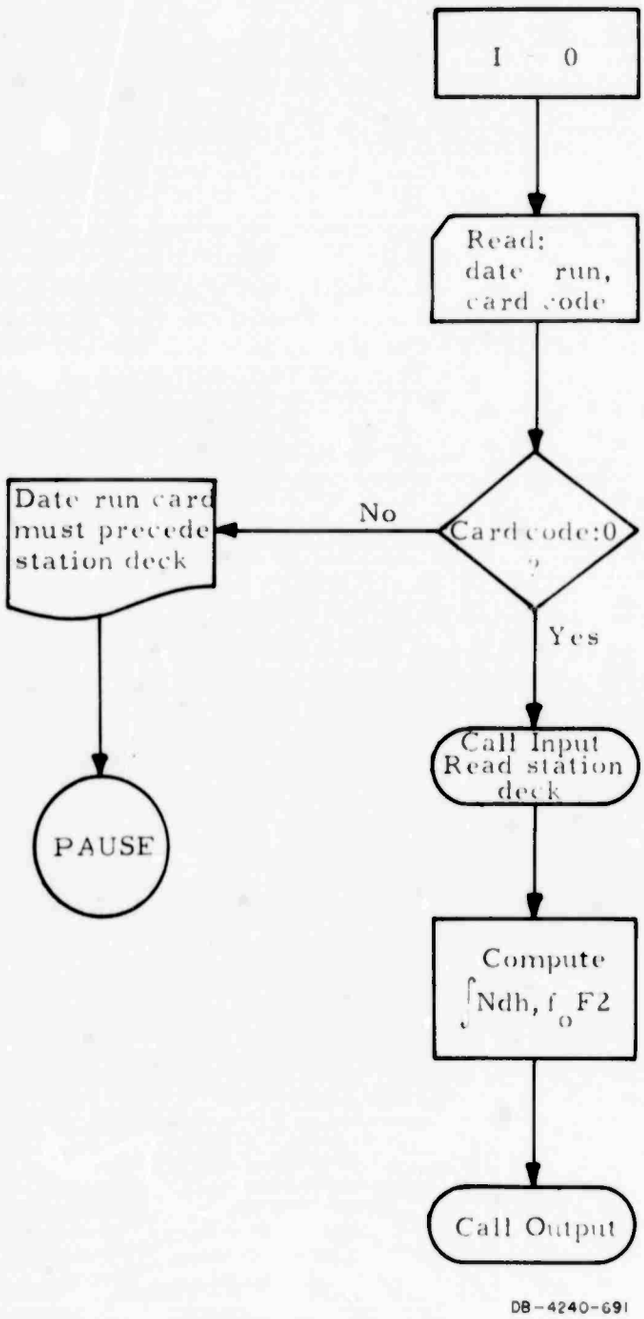

FIG. B-1 PROGRAM FLOWCHART

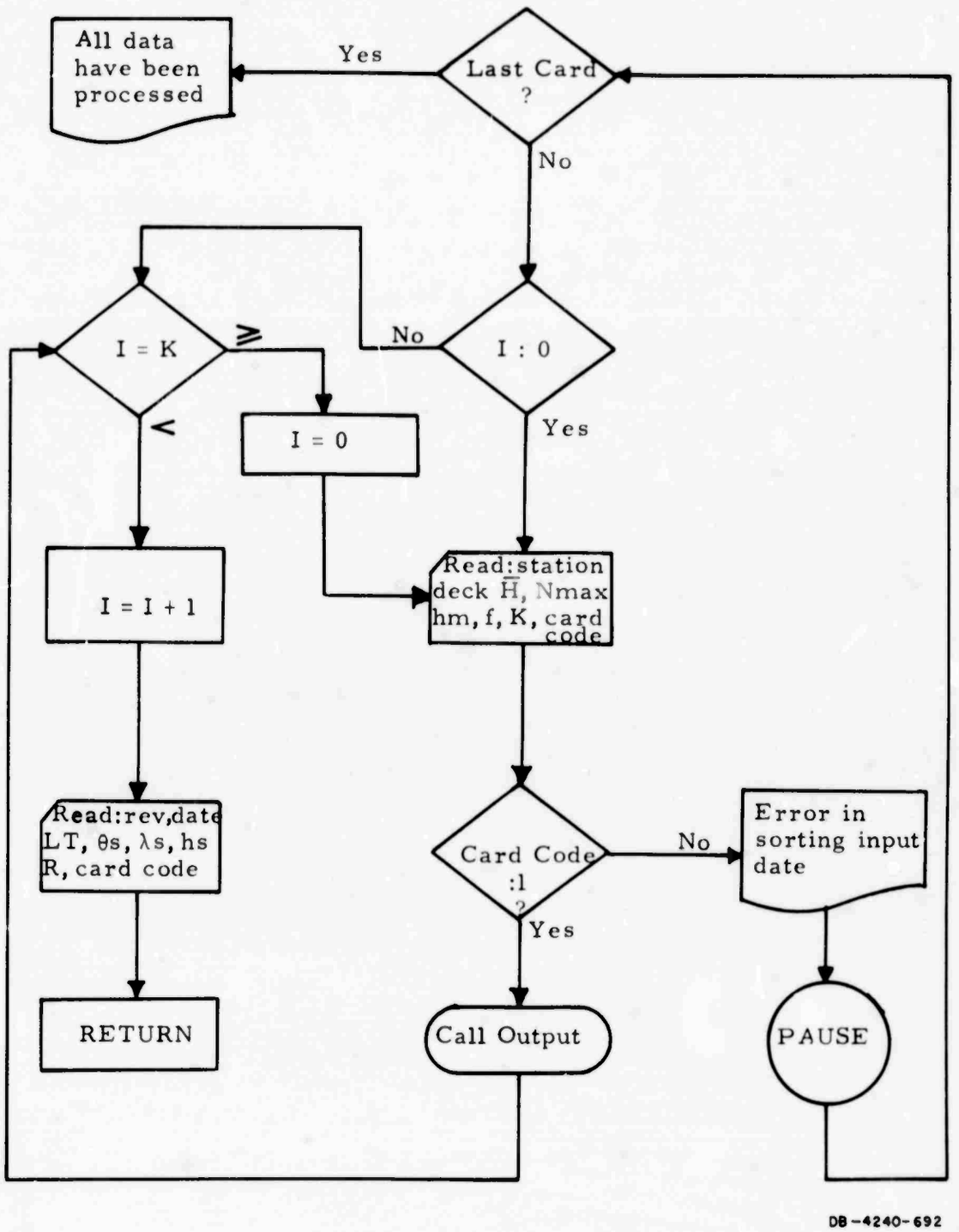

FIG. B-2 SUBROUTINE INPUT

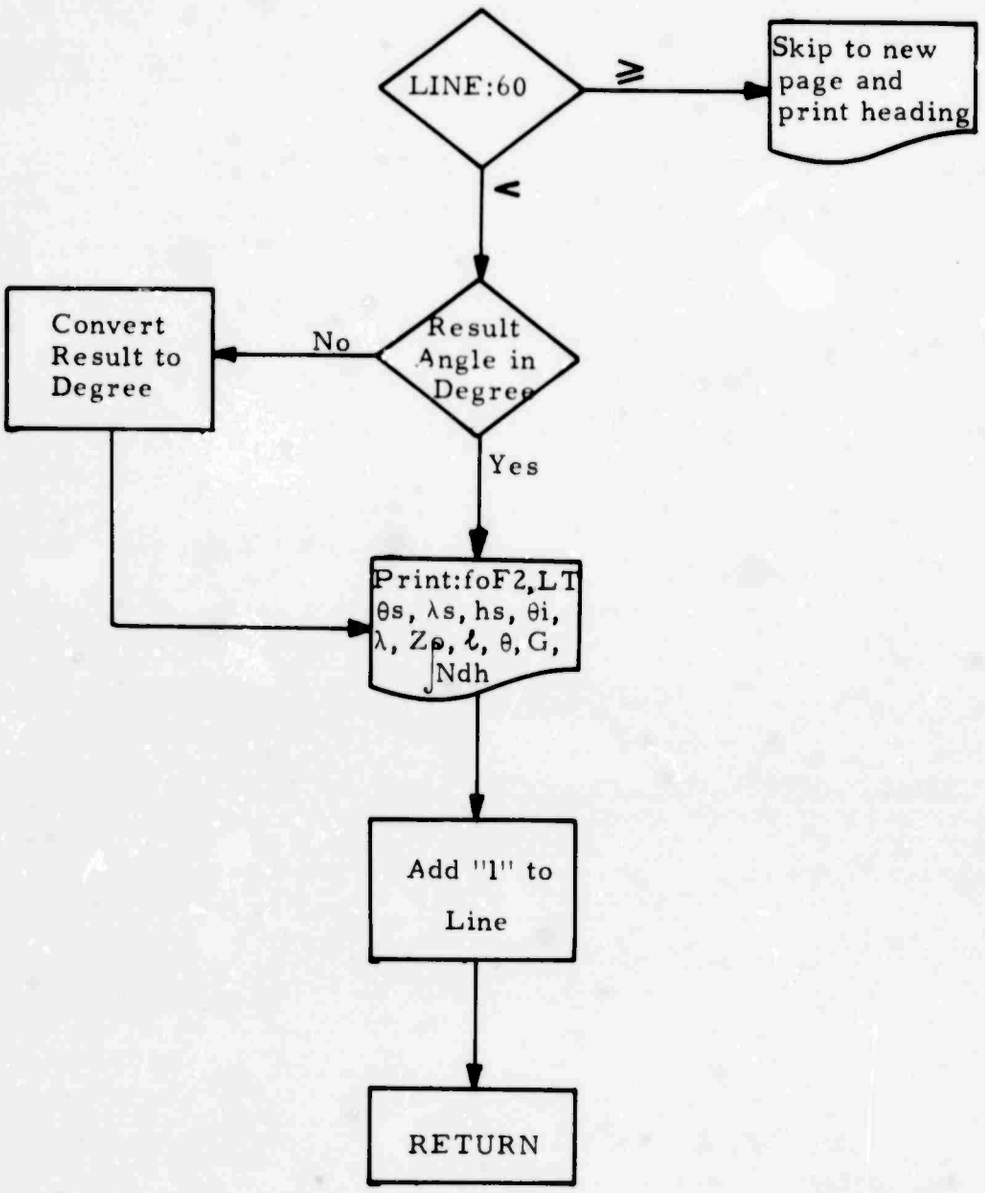

FIG. B-3 SUBROUTINE OUTPUT

Appendix C

SELECTED SATELLITE EPHEMERIS

Appendix C

SELECTED SATELLITE EPHEMERIS

Hour Group	Curve Number	Date	Revolution Number*	Observing Time
0000-0100	1	15 January 1967	11357D	0055
	2	22 January 1967	11453D	0040
0100-0200	1	20 January 1967	11426D	0130
0200-0300	1	7 January 1967	11248D	0230
	2	8 January 1967	11262D	0300
	3	10 January 1967	11289D	0210
0400-0500	1	4 October 1966	09944A	0405
	2	20 December 1966	11003D	0450
0600-0700	1	5 December 1966	10798D	0645
	2	8 December 1966	10839D	0620
	3	9 December 1966	10853D	0650
	4	11 December 1966	10880D	0600
	5	13 December 1966	10908D	0700
	6	19 December 1966	10990D	0610
	7	5 March 1967	12034A	0650
0700-0800	1	29 November 1966	10715D	0730
	2	7 December 1966	10826D	0745
	3	2 March 1967	11993A	0710
	4	3 March 1967	12007A	0740
	5	6 March 1967	12048A	0710
	6	7 March 1967	12062A	0740
0800-0900	1	28 November 1966	10702A	0850
	2	30 November 1966	10729D	0800
	3	1 December 1966	10744D	0830

*The letters A and D indicate ascending and descending satellite passes, respectively.

SELECTED SATELLITE EPHEMERIS - Continued

Hour Group	Curve Number	Date	Revolution Number*	Observing Time
	4	22 February 1967	11884D	0850
	5	25 February 1967	11925A	0820
	6	26 February 1967	11939A	0850
	7	28 February 1967	11966A	0800
	8	1 March 1967	11980A	0830
	9	4 March 1967	12021A	0800
0900-1000	1	15 February 1967	11788A	0900
	2	16 February 1967	11802A	0930
	3	20 February 1967	11857A	0930
	4	23 February 1967	11898A	0910
1000-1100	1	17 February 1967	11816A	1000
1100-1200	1	4 February 1967	11638A	1105
	2	5 February 1967	11652A	1130
1200-1300	1	6 February 1967	11666A	1200
1300-1400	1	15 January 1967	11365A	1410
	2	20 January 1967	11433A	1300
	3	21 January 1967	11447A	1330
1400-1500	1	8 January 1967	11269A	1430
1500-1600	1	10 January 1967	11297A	1625
1700-1800	1	19 December 1966	10997A	1740
1800-1900	1	13 December 1966	10915A	1830
	2	14 December 1966	10929A	1850
	3	20 December 1966	11011A	1810
	4	6 March 1967	12054D	1825
	5	9 March 1967	12095D	1810

*The letters A and D indicate ascending and descending satellite passes, respectively.

SELECTED SATELLITE EPHEMERIS - Continued

Hour Group	Curve Number	Date	Revolution Number*	Observing Time
1900-2000	1	4 December 1966	10792A	1930
	2	7 December 1966	10833A	1910
	3	8 December 1966	10847A	1930
	4	5 March 1967	12041D	1940
2000-2100	1	29 November 1966	10709A	2020
	2	25 November 1966	10668A	2040
	3	1 December 1966	10751A	2000
	4	16 February 1967	11808D	2050
	5	2 March 1967	12000D	2010
2100-2200	1	30 November 1966	10737A	2115
	2	13 February 1967	11767D	2110
	3	14 February 1967	11781D	2140
	4	17 February 1967	11822D	2110
2200-2300	1	11 February 1967	11740D	2200
2300-0000	1	5 November 1967	10395A	2350

*The letters A and D indicate ascending and descending satellite passes, respectively.

Appendix D

CALCULATED AND OBSERVED F-LAYER CRITICAL-FREQUENCY (foF2) VALUES

BLANK PAGE

Appendix D

CALCULATED AND OBSERVED F-LAYER CRITICAL FREQUENCY (foF2) VALUES

Hour Group	Curve Number	Date	Revolution Number*	Songkhla foF2 (MHz)			Bangkok foF2 (MHz)			Chiengmai foF2 (MHz)		
				Cal**	Obs	Error (%)	Cal	Obs	Error (%)	Cal	Obs	Error (%)
0000-0100	1	15 January 1967	11357D	5.0	4.5	-11.1	5.5	5.9	+6.7	6.1	---	---
	2	22 January 1967	11453D	6.7	---	---	7.0	6.9	-1.4	7.3	7.5	+2.6
0100-0200	1	20 January 1967	11426D	---	---	---	4.8	4.6	-4.3	---	---	---
0200-0300	1	7 January 1967	11248D	4.7	5.0	+6.0	4.3	4.4	-9.0	---	---	---
	2	8 January 1967	11262D	5.0	5.5	+9.0	4.1	3.6	-12.8	---	---	---
	3	10 January 1967	11289D	5.2	5.0	-4.0	5.3	5.5	+3.6	---	---	---
0400-0500	1	4 October 1966	09944A	2.4	---	---	1.9	2.0	+5.0	---	---	---
	2	20 December 1966	11003D	4.3	4.8	+10.4	3.8	3.4	-11.7	3.6	---	---
0600-0700	1	5 December 1966	10798D	6.8	---	---	5.7	5.5	-3.6	4.9	5.0	+2.0
	2	8 December 1966	10839D	5.2	5.0	-4.0	4.3	4.0	-7.5	3.4	---	---
	3	9 December 1966	10853D	6.4	---	---	5.7	5.6	-1.7	4.6	5.0	+8.0
	4	11 December 1966	10880D	4.0	4.3	+6.9	3.4	3.0	-13.3	3.1	3.0	-3.3

*The letters A and D indicate ascending and descending satellite passes.

**Cal = Calculated Values

Obs = Observed Values

\+ Observed values are higher than calculated

\- Observed values are lower than calculated.

CALCULATED AND OBSERVED F-LAYER CRITICAL FREQUENCY (foF2) VALUES - Continued

Hour Group	Curve Number	Date	Revolution Number*	Songkhla foF2 (MHz)			Bangkok foF2 (MHz)			Chiengmai foF2 (MHz)		
				Cal**	Obs	Error (%)	Cal	Obs	Error (%)	Cal	Obs	Error (%)
	5	13 December 1966	10908D	6.7	6.0	-11.6	5.5	5.4	-1.8	4.4	4.3	-2.3
	6	19 December 1966	10990D	4.4	---	---	4.7	4.6	-2.1	3.8	---	---
	7	5 March 1967	12034A	---	---	---	5.9	6.1	+3.2	6.0	6.0	0
0700-0800	1	29 November 1966	10715D	8.4	8.0	-5.0	8.4	8.0	-5.0	7.4	7.3	-1.3
	2	7 December 1966	10826D	6.6	7.2	+8.3	6.8	6.4	-6.2	5.9	6.3	+5.3
	3	2 March 1967	11993A	---	---	---	7.2	---	---	6.9	6.5	-6.1
	4	3 March 1967	12007A	9.1	9.5	+4.2	9.1	9.0	-1.1	8.9	9.5	+6.3
	5	6 March 1967	12048A	8.5	9.0	+5.5	8.4	8.7	+3.4	8.1	8.0	-1.2
	6	7 March 1967	12062A	9.4	9.8	+4.0	9.9	10.0	+1.0	9.6	9.5	-1.0
0800-0900	1	28 November 1966	10702A	8.1	8.0	-1.2	8.7	9.2	+5.4	8.3	8.9	+6.7
	2	30 November 1966	10729D	8.8	8.5	-3.5	8.9	9.3	+4.3	7.8	8.0	+2.5
	3	1 December 1966	10744D	8.9	8.0	-11.2	9.5	9.4	-1.0	9.0	10.0	+10.0
	4	22 February 1967	11884D	10.2	10.0	-2.0	10.7	10.9	+1.8	9.7	10.5	+7.6
	5	25 February 1967	11925A	10.0	10.2	+1.9	10.9	10.8	-0.9	10.0	10.0	0

* The letters A and D indicate ascending and descending satellite passes.
**Cal = Calculated Values
Obs = Observed Values
+ Observed values are higher than calculated.
- Observed values are lower than calculated.

CALCULATED AND OBSERVED F-LAYER CRITICAL FREQUENCY (foF2) VALUES - Continued

Hour Group	Curve Number	Date	Revolution Number*	Songkhla foF2 (MHz)			Bangkok foF2 (MHz)			Chiengmai foF2 (MHz)		
				Cal**	Obs	Error (%)	Cal	Obs	Error (%)	Cal	Obs	Error (%)
	6	26 February 1967	11939A	11.1	11.2	+0.8	12.0	11.8	-1.6	11.1	12.0	+7.5
	7	28 February 1967	11966A	9.2	9.5	+3.1	9.5	9.3	-2.1	8.6	9.0	+4.4
	8	1 March 1967	11980A	10.6	10.0	-6.0	10.7	10.7	0	10.0	10.5	+4.7
	9	4 March 1967	12021A	9.8	10.0	+2.0	10.2	10.4	+1.9	9.6	10.0	+4.0
0900-1000	1	15 February 1967	11788A	10.1	10.3	+1.9	10.3	10.4	+0.9	9.7	11.0	+11.8
	2	16 February 1967	11802A	9.4	9.0	-4.4	9.9	9.8	-1.0	10.1	11.0	+8.1
	3	20 February 1967	11857A	10.1	10.0	-1.0	11.3	11.1	-1.8	10.5	11.0	+4.5
	4	23 February 1967	11898A	11.1	11.0	-0.9	12.3	11.8	-4.2	11.3	11.5	+1.7
1000-1100	1	17 February 1967	11816A	9.0	10.0	+10.0	10.4	10.2	-1.9	10.8	11.0	+1.8
1100-1200	1	4 February 1967	11638A	10.5	---	---	12.0	11.4	-5.2	12.3	13.0	+5.3
	2	5 February 1967	11652A	10.7	---	---	12.4	12.2	-1.6	11.1	12.5	+11.2
1200-1300	1	6 February 1967	11666A	10.2	---	---	10.8	10.5	-2.8	13.4	14.2	+5.6
1300-1400	1	15 January 1967	11365A	8.0	8.1	+1.2	8.0	8.3	+3.6	9.1	9.0	-1.1
	2	20 January 1967	11433A	---	---	---	9.2	8.8	-4.5	10.5	11.2	+6.2
	3	21 January 1967	11447A	8.8	8.0	-10.0	8.7	7.9	-10.1	10.6	11.3	+6.1

*The letters A and D indicate ascending and descending satellite passes.

**Cal = Calculated Values

Obs = Observed Values

\+ Observed values are higher than calculated.

\- Observed values are lower than calculated.

CALCULATED AND OBSERVED F-LAYER CRITICAL FREQUENCY (foF2) VALUES - Continued

Hour Group	Curve Number	Date	Revolution Number*	Songkhla foF2 (MHz)			Bangkok foF2 (MHz)			Chiengmai foF2 (MHz)		
				Cal**	Obs	Error (%)	Cal	Obs	Error (%)	Cal	Obs	Error (%)
1400-1500	1	8 January 1967	11269A	11.4	12.3	+7.3	12.0	10.4	-15.3	---	---	---
1500-1600	1	10 January 1967	11297A	9.0	9.0	0	9.6	9.5	-1.0	---	---	---
1700-1800	1	19 December 1966	10997A	10.4	10.0	-4.0	11.0	10.5	-4.7	11.7	12.7	+7.8
1800-1900	1	13 December 1966	10915A	8.2	9.0	+8.8	9.5	9.6	+1.0	8.7	9.0	+3.3
	2	14 December 1966	10929A	10.6	11.0	+3.6	11.7	11.6	-0.8	10.0	9.5	-5.2
	3	20 December 1966	11011A	9.9	9.5	-4.2	11.3	11.0	-2.7	11.7	13.0	+10.0
	4	6 March 1967	12054D	8.0	---	---	8.9	8.8	-1.1	---	---	---
	5	9 March 1967	12095D	9.8	10.5	+6.6	10.2	10.1	-0.9	12.2	---	---
1900-2000	1	4 December 1966	10792A	9.0	9.5	+5.2	9.1	8.8	-3.4	8.5	9.0	+5.5
	2	7 December 1966	10833A	8.4	8.5	+1.1	10.2	9.5	-7.3	10.3	---	---
	3	8 December 1966	10847A	7.6	8.0	+5.0	9.6	10.6	+9.4	8.7	9.5	+8.4
	4	5 March 1967	12041D	8.0	---	---	9.5	9.0	-5.5	---	---	---

*The letters A and D indicate ascending and descending satellite passes.

**Cal = Calculated Values
Obs = Observed Values
+ Observed values are higher than calculated.
- Observed values are lower than calculated.

CALCULATED AND OBSERVED F-LAYER CRITICAL FREQUENCY (foF2) VALUES - Continued

Hour Group	Curve Number	Date	Revolution Number*	Songkhla foF2 (MHz)			Bangkok foF2 (MHz)			Chiengmai foF2 (MHz)		
				Cal**	Obs	Error (%)	Cal	Obs	Error (%)	Cal	Obs	Error (%)
2000-2100	1	29 November 1966	10709A	10.4	10.2	-1.9	9.7	9.7	0	8.1	7.8	-3.8
	2	25 November 1966	10668A	8.9	9.0	+1.1	8.9	0	-8.1	8.5	8.8	+3.4
	3	1 December 1966	10751A	9.1	9.0	-1.1	10.0	9.1	-9.8	9.4	10.5	+10.4
	4	16 February 1967	11808D	8.2	9.0	+8.8	9.6	9.4	-2.1	---	---	---
	5	2 March 1967	12000D	7.4	7.9	+6.3	7.8	8.3	+6.0	8.4	---	---
2100-2200	1	30 November 1966	10737A	8.6	9.6	+10.4	9.4	9.3	-1.0	9.2	9.0	-2.2
	2	13 February 1967	11767D	7.6	8.8	+13.6	9.4	9.8	+4.0	11.0	---	---
	3	14 February 1967	11781D	7.2	6.5	-10.7	8.8	9.0	+2.2	10.8	10.5	-2.8
	4	17 February 1967	11822D	8.4	8.0	-5.0	9.9	9.5	-4.2	14.5	14.0	-3.5
2200-2300	1	11 February 1967	11740D	9.1	10.0	+9.0	10.0	10.8	+7.4	11.6	---	---
2300-0000	1	5 November 1967	10395A	7.2	6.4	-11.1	8.6	9.0	+4.4	---	---	---
Mean of absolute value of error						5.3			4.2			5.0

*The letters A abd D indicate ascending and descending satellite passes.
**Cal = Calculated Values
Obs = Observed Values
+ Observed Values are higher than calculated.
- Observed values are lower than calculated.

BLANK PAGE

REFERENCES

1. Vichai T. Nimit, Boonsong Punyarut, and C. L. Rufenach, "Faraday Rotation Data: Bangkok, Thailand, Reporting Period: November 1964-June 1965," Geophysical Data Report, SRI Project 4240, Contract DA 36-039 AMC-00040(E), Stanford Research Institute, Menlo Park, California. (February 1966).

2. Vichai T. Nimit, Boonsong Punyarut, and C. L. Rufenach, "Faraday Rotation Data: Bangkok, Thailand, Reporting Period: July-December 1965," Geophysical Data Report, SRI Project 4240, Contract DA 36-039 AMC-00040(E), Stanford Research Institute, Menlo Park, California (May 1966).

3. Vichai T. Nimit, "Faraday Rotation Data: Bangkok, Thailand, Reporting Period: January-June 1966," Geophysical Data Report, SRI Project 4240, Contract DA 36-039 AMC-00040(E), Stanford Research Institute, Menlo Park, California (July 1966).

4. Vichai T. Nimit, "Faraday Rotation Data: Bangkok, Thailand, Reporting Period: July-December 1966," Geophysical Data Report, SRI Project 4240, Contract DA 36-039 AMC-00040(E), Stanford Research Institute, Menlo Park, California (January 1967).

5. Vichai T. Nimit, "Faraday Rotation Data: Bangkok, Thailand, Reporting Period: January-June 1967," Geophysical Data Report, SRI Project 4240, Contract DA 36-039 AMC-00040(E), Stanford Research Institute, Menlo Park, California (July 1967).

6. C. L. Rufenach, Vichai T. Nimit, and R. E. Leo, "Faraday Rotation Measurements of Electron Content near the Magnetic Equator Using the Transit IV-A Satellite," Special Technical Report 14, Contract DA 36-039 AMC-00040(E), SRI Project 4240, Stanford Research Institute, Menlo Park, California, pp. 1-8 (January 1966).

7. J. A. Ratcliffe, The Magneto-Ionic Theory and Its Applications to Ionosphere (Cambridge University Press, 1959).

8. K. C. Yeh, and V. H. Gonzalez, "Note on the Geometry of the Earth Magnetic Field Useful to Faraday Effect Experiments," J. Geophys. Research, Vol. 65, pp. 3209-3214 (1960).

9. P. A. Arendt, A. Papayaonov, and H. Soicher, "Determination of the Ionospheric Electron Content Utilizing Satellite Signals," Proc. IEEE, Vol. 53, pp. 268 (1965).

10. J. V. Evans, "Cause of the Midlatitude Winter Night Increase in foF2," J. Geophys. Research, Vol. 70, pp. 4331-4345 (1965).

11. G. O. Walker and Chan Tin, "Studies of the Ionosphere Using Radio Signals from Satellites," Physics Department, University of Hong Kong. Paper presented at Pacific Science Congress, Tokyo, Japan, August 1966.

12. N. Narayana Rao, "Ionospheric Electron Content and Irregularities Deduced from BE-C Satellite Transmissions," J. Geophys. Research, Vol. 72, pp. 2929-2942 (1967).

13. J. W. Wright, "A Model of the F Region Above hmF2," J. Geophys. Research, Vol. 65, pp. 185-191 (1960).

14. B. C. Potts, "Mean Ionospheric Scale Heights Deduced from Faraday Rotation Measurements," J. Geophys. Research, Vol. 70, pp. 2651-2663 (1965).

15. E. O. Olatunji, "The Total Electron Content of the Equatorial Ionosphere," J. Atmos, and Terrest. Phys., Vol. 29, pp. 285-299 (1967).

16. J. W. King, E. O. Olatunji, D. Eccles, and W. S. Newman, "The Integrated Electron Content in the Equatorial Ionosphere," J. Atmos. and Terrest. Phys., Vol. 29, pp. 1391-1396 (1967).

17. R. S. Lawrence and C. G. Little, "On the Analysis of Polarization Rotation Recordings of Satellite Radio Signals," Proceeding of Symposium Organized by the URSI/AGI Committee at Brussels, Belgium, September 1959, Elsevier Publishing Company, pp. 391-399.

18. L. J. Blumle, "Studies of Equatorial Ionosphere Using the Faraday Effect on Satellite Radio Transmissions," Scientific Report No. 156, Ionosphere Research Laboratory, Satellite Project, Pennsylvania State University (March 1961).

19. E. Golton, "A Method for the Analysis of Combined Faraday and Differential Doppler Recordings in the Presence of Horizontal Gradients and Vertical Satellite Motion," J. Atmos. and Terrest. Phys., Vol. 24, pp. 554-558 (1962).

20. C. G. Little and R. S. Lawrence, "The Use of the Polarization Fading of Satellite Signals to Study the Electron Content and Irregularities of the Ionosphere," J. Research NBS 64D, pp. 335-346 (1960).

21. K. Davies, "Ionospheric Radio Propagation," NBS Monograph 80, pp. 125-129, National Bureau of Standards, Boulder, Colorado (April 1965).

22. R. A. Goldberg, P. C. Kendall, and E. R. Schmerging, "Geomagnetic Control of the Electron Density of the F-Region of the Ionosphere," J. Geophys. Research, Vol. 69, pp. 417-427 (1964).

23. J. W. Wright, "A Model of the F-Region above hmF2," J. Geophys. Research, Vol. 65, pp. 185-191 (1960).

24. J. O. Thomas, M. J. Ryeroft, and K. L. Chan, "Experiment Results from the Alouette I Satellite," Proceedings of the NATO Advanced Study Institute held at Fine, Norway, April 1965, pp. 321-357 (North-Holland Publishing Company-Amsterdam, 1966).

25. C. L. Rufenach and G. H. Hagn, "Comparison of C-2 Ionospheric Sounder Data with Frequency Predictions for Short-Range Communication with Manpack Transceivers in Thailand," Special Technical Report 15, Contract DA 36-039 AMC-00040(E), SRI Project 4240, Stanford Research Institute, Menlo Park, California (August 1966).

26. C. L. Rufenach, "Evaluation and Prediction of Maximum Usable Frequency (MUF) Over Bangkok," Special Technical Report 28, Contract DA 36-039 AMC-00040(E), SRI Project 4240, Stanford Research Institute, Menlo Park, California (January 1967).

27. D. J. Barnes and J. Chapman, "Geomagnetic Data: Bangkok, Thailand, January-March 1966," Geophysical Data Report, Contract DA 36-039 AMC-00040(E), SRI Project 4240, Stanford Research Institute, Menlo Park, California (March 1967).

28. Vichai T. Nimit, "Measurements of Equatorial Magnetic Dip Angle at Ionospheric Heights," Special Technical Report 33, Contract DA 36-039 AMC-00040(E), SRI Project 4240, Stanford Research Institute, Menlo Park, California (May 1967).

UNCLASSIFIED

Security Classification

DOCUMENT CONTROL DATA · R & D

Security classification of title, body of abstract and indexing annotation must be entered when the overall report is classified

1. ORIGINATING ACTIVITY (Corporate author) Stanford Research Institute Menlo Park, California	2a. REPORT SECURITY CLASSIFICATION UNCLASSIFIED 2b. GROUP N/A

3. REPORT TITLE

MEASUREMENTS OF ELECTRON CONTENT AND LATITUDINAL F-LAYER CRITICAL FREQUENCY NEAR THE MAGNETIC EQUATOR

4. DESCRIPTIVE NOTES (Type of report and inclusive dates)

Special Technical Report 34

5. AUTHOR(S) (First name, middle initial, last name)

Vichai T. Nimit

6. REPORT DATE December 1967	7a. TOTAL NO. OF PAGES 108	7b. NO. OF REFS 28
8a. CONTRACT OR GRANT NO Contract DA 36-039 AMC-00040(E) b. PROJECT NO Order No. 5384-PM-63-91 c. ARPA Order 371 d	9a. ORIGINATOR'S REPORT NUMBER(S) Special Technical Report 34 SRI Project 4240 9b. OTHER REPORT NO(S) (Any other numbers that may be assigned this report)	

10. DISTRIBUTION STATEMENT

Distribution of this document is unlimited

11. SUPPLEMENTARY NOTES	12. SPONSORING MILITARY ACTIVITY Advanced Research Projects Agency Washington, D.C.

13. ABSTRACT

Faraday rotation data from Satellite S-66 were accumulated at the Electronics Laboratory of the Military Research and Development Center, Bangkok, Thailand from November 1964 through June 1967, a period of intermediate sunspot number (sunspot minimum condition at 1964/1965 and sunspot maximum condition at 1968/1969). These data provide a means of improving ionospheric frequency predictions for regions in Thailand remote from Bangkok (i.e., where no ionosonde data are available).

In this report, two methods of analysis--involving rotation rate and total number of rotations--are applied to the Bangkok observations. The rotation-rate method is used to determine the electron content when the angle between the ray path and geomagnetic field is 90° (transverse position). The total-rotations method is used to determine latitudinal variations of electron content of the equatorial ionosphere for the selected passes from a joint analysis of observations at three stations in Thailand--Songkhla, Bangkok, and Chiengmai.

The diurnal variation of the local electron content shows low early-morning values and high afternoon values, resulting in a large maximum-to-minimum ratio. A secondary maximum was observed during the nighttime. The diurnal and seasonal variations of electron content are examined together with the variation with solar activity as measured by the 10.7-cm solar radio flux.

The diurnal development and collapse of the equatorial anomaly in electron content is clearly seen from the total-rotations data. The Chapman equation is used for conversion of these total electron content values to peak electron density in order to compute the F-layer critical frequency (foF2) and its variation as a continuous function of latitude. The computed foF2 values are compared with those obtained from three ionosondes which were located at Songkhla, Bangkok, and Chiengmai, and the agreement is typically within 10 percent.

DD FORM 1 NOV 65 1473 (PAGE 1)

S/N 0101-807-6801

UNCLASSIFIED

Security Classification

14 KEY WORDS	LINK A		LINK B		LINK C	
	ROLE	WT	ROLE	WT	ROLE	WT
Faraday rotation effect						
Rotation rate						
Total rotations						
Magnetic equator						
Ionospheric electron content						
Latitudinal variation						
Diurnal variation						
Explorer 22 (S-66)						
Ionospheric scale height						
Equatorial anomaly						
F-layer critical frequency vs. latitude						
Transequatorial ionosphere						
Bangkok, Chiengmai, and Songkhla, Thailand						
Southeast Asia						
SEACORE						